CHEMISTRY
A EUROPEAN JOURNAL

DOI: 10.1002/chem.200802152

Solvent-Assisted Organized Structures Based on Amphiphilic Anion-Responsive π-Conjugated Systems

Hiromitsu Maeda,*[a, b] Yoshihiro Ito,[a] Yohei Haketa,[a] Nazuki Eifuku,[a] Eunji Lee,[c] Myongsoo Lee,[c] Takeshi Hashishin,[d] and Kenji Kaneko[e]

Abstract: The synthesis of amphiphilic π-conjugated acyclic oligopyrroles and the formation of solvent-assisted aggregates are reported. We have prepared various types of BF_2 complexes of 1,3-dipyrrolylpropane-1,3-diones bearing aryl rings substituted with hydrophilic polyethyleneglycol (PEG) chains, both as acyclic anion receptors and as building subunits for organized architectures based on π–π stacking. The formation of supramolecular H-type assemblies of these "amphiphilic" derivatives in aqueous solution was suggested by UV/Vis and fluorescence spectroscopy and further supported by ^{1}H NMR and dynamic light scattering (DLS) analyses. Cryogenic transmission electron microscopy (cryo-TEM) analyses of the aqueous solutions suggest that the fabrication of nanoscale network structures and vesicles depends on the peripheral substituents. The H-aggregates in aqueous solution are sensitive to the conditions required for transformation into monomers through replacement with miscible solvents such as alcohols and into J-type aggregates by water evaporation and freeze-drying procedures. However, they are fairly stable and sustainable to anion binding, whereas on CH_2Cl_2 extraction they are transformed into other assembled modes but remain in the aqueous solution. The metastable states of affairs for distributions between two immiscible solvents are controlled by the orders of solution preparation; this also suggests that the formation of stable assemblies is assisted by water molecules. Furthermore, assemblies in which the stacking modes depend on the aliphatic side chains are also observed in a nonpolar hydrocarbon solvent.

Keywords: amphiphiles · H-aggregates · pyrrole derivatives · supramolecular chemistry · vesicles

Introduction

Supramolecular assemblies in aqueous solution are ubiquitously observed in biotic systems, including in protein folding, DNA double helices, membranes consisting of lipid bilayers, etc.[1] These organized structures can be formed through the interactions between hydrophobic moieties inside the assemblies and the association of hydrophilic sites with water molecules.[2] In artificial systems, various amphiphilic molecules have been observed to form ordered aggregates in the solution state.[3–6]

Among the building subunits used for supramolecular assemblies, π-conjugated systems bearing hydrophilic (and also aliphatic) chains are useful for the formation of nanoscale architectures through stacking of π-planes, which also act as hydrophobic moieties, especially in aqueous solution. Lee et al., for example, have reported oligophenylene derivatives and their analogues that self-assemble to form nanofibers and nanosheets that act as liquid crystals and supramolecular gels, and also as micelles and multilayer vesicles.[3] On the other hand, Fukushima and Aida et al. have report-

[a] Prof. Dr. H. Maeda, Y. Ito, Y. Haketa, N. Eifuku
College of Pharmaceutical Sciences
Institute of Science and Engineering
Ritsumeikan University, Kusatsu 525-8577 (Japan)
Fax: (+81) 77-561-2659
E-mail: maedahir@ph.ritsumei.ac.jp

[b] Prof. Dr. H. Maeda
PRESTO, Japan Science and Technology Agency (JST)
Kawaguchi 332-0012 (Japan)

[c] E. Lee, Prof. Dr. M. Lee
Center for Supramolecular Nanoassembly
and Department of Chemistry
Yonsei University, Seoul 120-749 (Korea)

[d] Dr. T. Hashishin
College of Life Sciences, Institute of Science and Engineering
Ritsumeikan University, Kusatsu 525-8577 (Japan)

[e] Prof. Dr. K. Kaneko
Department of Materials Science and Engineering
Graduate School of Engineering, Kyushu University
Fukuoka 819-0395 (Japan)

Supporting information for this article is available on the WWW under http://dx.doi.org/10.1002/chem.200802152.

ed that self-assembly of amphiphilic hexabenzocoronenes produces π-electronic, discrete nanotubular objects.[4] Furthermore, Würthner et al. have also reported morphology control of nanoaggregates governed by the shapes of amphiphilic perylene bisimides.[5] Dynamic conformation changes in amphiphilic aggregates resulting from changes in ambient conditions are fascinating from the point of view of their potential applications as soft materials in aqueous solutions. Therefore, organized structures that can be modulated by external physical and chemical stimuli[6] such as temperature,[6c] solvents,[6d] provide versatile actuators that can be activated in aqueous solutions and related solvents.

As scaffoldings for the formation of organized structures based on π–π stacking interactions, we have reported acyclic planar π-conjugated systems in the form of BF_2 complexes of 1,3-dipyrrolylpropane-1,3-diones (e.g., **1a–c**, Scheme 1a),[7–9] which are anion receptors[10–12] based on two pyrrole NH components joined by bridging CH units, in which anion binding is governed by the inversion of pyrrole rings (Scheme 1b). In fact, α-aryl-substituted receptors incorporating long aliphatic chains, such as **1b** or **1c**, constitute anion-responsive supramolecular organogels obtained from octane solutions and exhibit transitions to the solution state on addition of appropriate anions.[12a] This result suggests that amphiphilic π-conjugated systems bearing hydrophilic substituents also form stacking structures in aqueous solution states, giving rise to organized structures potentially responsive to stimuli such as anions, temperature, and solvents.

In this article we report the syntheses of amphiphilic π-conjugated acyclic oligopyrroles (**2a–d** and **3a–d**; Scheme 1c,d), which in aqueous solution give rise to solvent-assisted assemblies such as nanoscale vesicles[13] based on H-aggregates; these water-assisted aggregates are stable and sustainable to external stimuli such as anions, whereas extraction with immiscible organic solvents or removal of water switches the assemblies into other stacking modes such as J-type aggregates.

Results and Discussion

Synthesis and characterization of amphiphilic C_3-bridged oligopyrroles: In this work two kinds of "amphiphilic" receptors were designed: a) derivatives based on hydrophilic chains and a hydrophobic π-plane, and b) derivatives incorporating both hydrophilic and aliphatic (hydrophobic) chains together with a hydrophobic π plane. We selected polyethyleneglycol (PEG) units as the neutral hydrophilic moieties.

As the precursors of amphiphilic anion receptors of type A, diketones **2a′–c′**, with two, four, and six triethyleneglycol (TEG) chains, respectively, and **2d′**, with six hexaethyleneglycol (HEG) substituents, at the 3,4,5-positions of their aryl rings were obtained in 26, 61, 56, and 24% yields, respectively, from the corresponding arylpyrroles (which were in turn synthesized through Suzuki cross-coupling reactions[14]) and malonyl chloride in CH_2Cl_2.[7–9,15] Subsequent treatment with $BF_3{\cdot}OEt_2$ led to the formation of the highly fluorescent BF_2 complexes **2a–d** (Scheme 1c) in moderate yields. Similarly, the "genuine" amphiphilic derivatives **3a–d** (type B; Scheme 1d), containing both hydrophilic and amphiphilic chains, were synthesized from the corresponding dipyrrolyldiketones **3a′–d′**, obtained by condensation of the two kinds of arylpyrroles and malonyl chloride. The initial characterization of **2a–d** and **3a–d** was performed by ^{1}H NMR and FAB-MS or ESI-TOF-MS analysis. These amphiphilic derivatives are soluble in ordinary organic solvents such as CH_2Cl_2. The absorption maxima (λ_{max}) of **2a–d** in CH_2Cl_2 are observed at 519, 503, 517, and 518 nm, respectively, whereas those of **3a–d** are observed at 519, 520, 519, and 519 nm, respectively (Figure S11 in the Supporting Information). These λ_{max} values are red-shifted in relation to the λ_{max} value of the α-phenyl derivative **1a** (500 nm),[10a] due to the electron-donating properties of the alkoxy groups. The fluorescence emissions (λ_{em} excited at each λ_{max}) and quantum yields (Φ_F) of **2a–d** in CH_2Cl_2 are observed at 557, 534, 558, and 559 nm (Φ_F = 0.94, 0.94, 0.78, and 0.68), respectively, whereas **3a–d** exhibit almost the same λ_{em} values: 564, 563, 564, and

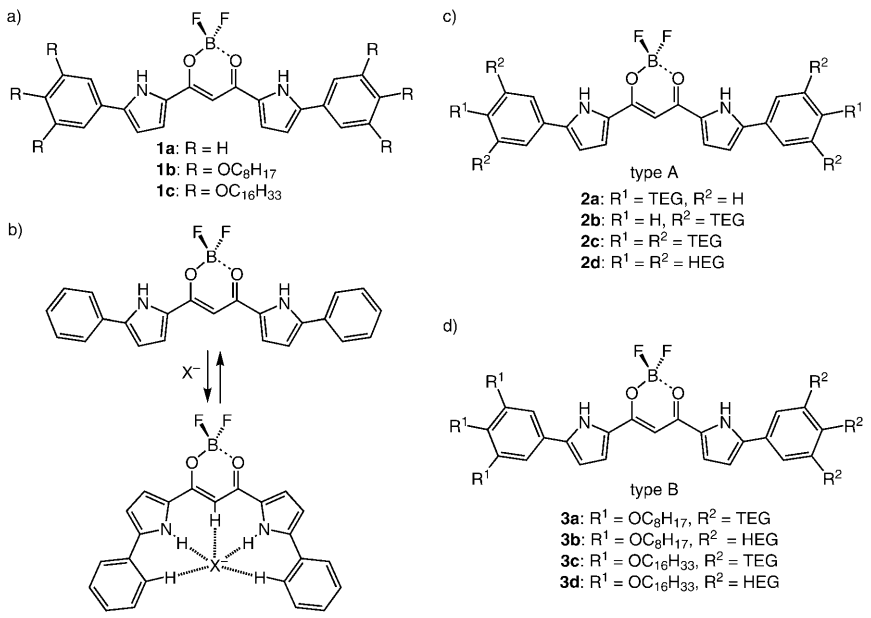

Scheme 1. a) BF_2 complexes of dipyrrolyldiketones **1a–c**. b) Anion binding mode of **1a**. c) Amphiphilic derivatives **2a–d** (type A). d) Amphiphilic derivatives **3a–d** (type B).

563 nm ($\Phi_F = 0.81$, 0.73, 0.81, and 0.72) (Figure S12 in the Supporting Information).

The structures of the amphiphilic receptors optimized by AM1 calculations show noticeably long molecules in the stable conformations, with linearly aligned PEG and aliphatic chains. The lengths of the molecules, for example, are about 37 Å for **2c**, 53 Å for **2d**, and 39 Å for **3a** (Figure S1 in the Supporting Information). The folding geometry of PEG[3,5,16] in the aqueous solution state, due to hydrogen bonding with water molecules, is well known, and contrasts with the straight (all-*trans*) geometries of alkyl chains. In the "preorganized" conformations of the amphiphilic molecules **2a–d** and **3a–d**, with the two inverted pyrrole rings, the hydrophilic (and hydrophobic) substituents are located so as to form hemi-cavities for anion binding.

Self-assembly of PEG-substituted anion receptors (type A) in aqueous solution: The self-assembly behavior of the amphiphilic receptors **2a–d** (type A) in aqueous solution was investigated. Whereas the bis-TEG-substituted **2a** exhibits precipitation in water, the derivatives **2b–d** are soluble in that solvent, in which their λ_{max} values are observed at 460, 496, and 506 nm (1×10^{-5} M), respectively, blue-shifted in relation to those in MeOH (498, 510, and 512 nm) (Figure 1), suggesting the formation of H-aggregates in aqueous solution. The absorption spectral changes of **2b–d** in mixed solvent systems of water and the miscible MeOH show sweeping "transitions" with increasing proportions of water: the sigmoidal curves observed in the transitions between monomers (in MeOH) and assemblies (in water) are due to the selective solvation for each state (monomers and assemblies) by MeOH and water, respectively. Moderate red shifts with small amounts of water are due to the increasing solvent polarity, which stabilizes the polarized excited state rather than the ground state. In each case, small amounts of monomers are observed as the shoulders around 500 nm—especially in the case of **2d**—in aqueous solutions. Furthermore, the formation of a tightly stacked assembly of **2b**, as opposed to those of **2c** and **2d**, is suggested by the shift values in the absorption spectral changes and the smaller ratio of water (ca. 70%) at the blue-shift transition; this is also supported by the broader nature of the ^{1}H NMR signals of **2b** relative to those of the fairly soluble **2c** and **2d** in D_2O (Figure S15 in the Supporting Information). The fluorescence spectra of **2b–d** in aqueous solution show peaks at 546, 571, and 572 nm (Figure S12 in the Supporting Informa-

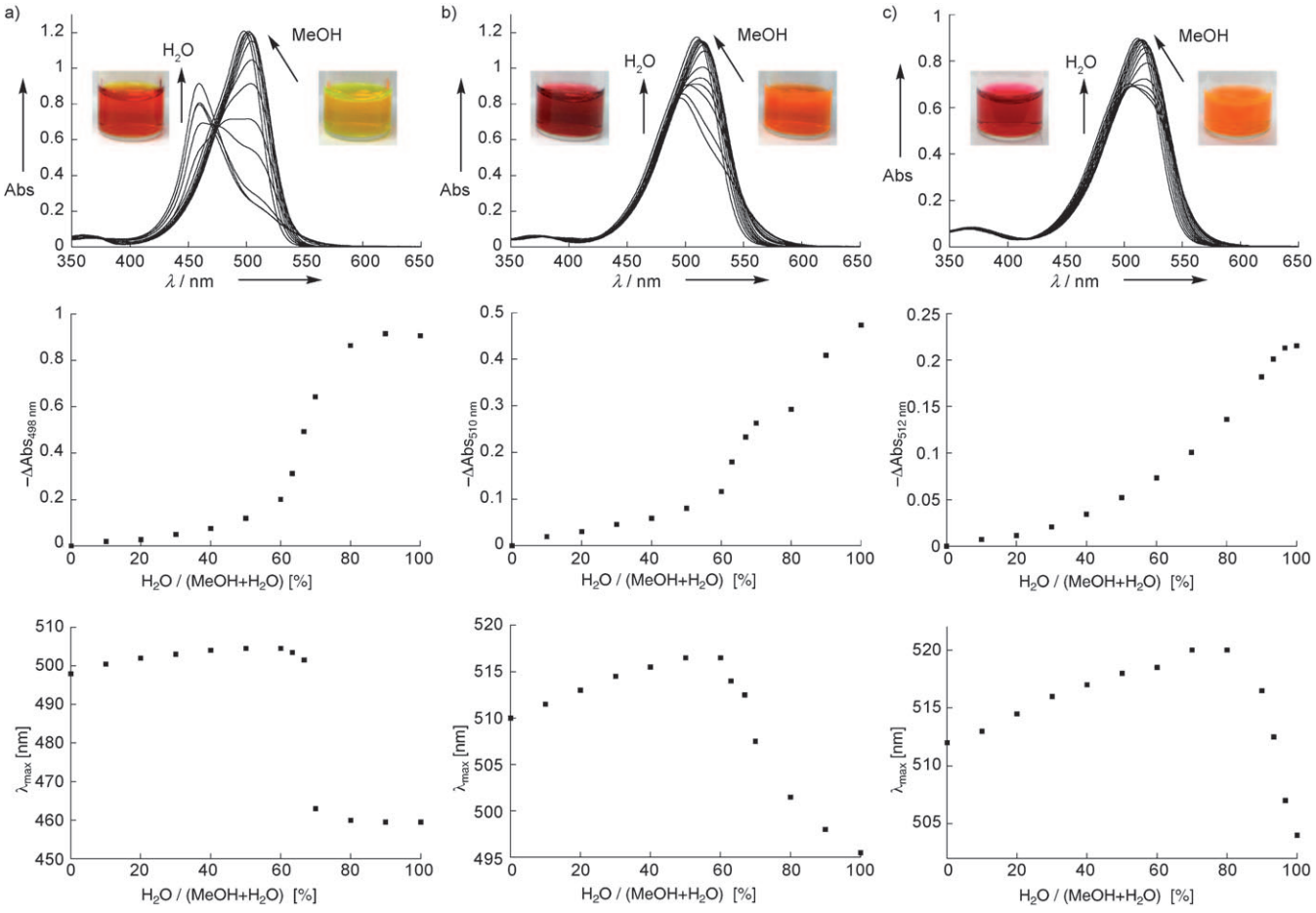

Figure 1. UV/Vis absorption spectral changes in H_2O/MeOH mixed solvents (1×10^{-5} M) and the color changes in H_2O and MeOH (insets, 5×10^{-4} M) (top), the changes in the absorbances at the λ_{max} in MeOH according to the proportion (*v*/*v*) of water (middle), and the changes in the λ_{max} values according to the proportion (*v*/*v*) of water (bottom): a) **2b**, b) **2c**, and c) **2d**.

tion) with low emission quantum yields (Φ_F, determined at λ_{ex}, which are equal to the corresponding λ_{max}) of 0.01, 0.01, and 0.09, respectively, which are characteristic features of H-aggregates. The emissions from the aqueous solution appear to originate from trace amounts of the monomeric species in water, as is suggested by the fairly sharp excitation spectrum of each emission maximum, with red-shifted λ_{max} values of 507 (**2b**), 524 (**2c**), and 529 nm (**2d**), relative to the absorption maxima in aqueous solution (460, 496, and 504 nm) as H-aggregates and to those in the less polar CH_2Cl_2 (503, 517, and 517 nm) as monomers (Figures S11 and S13 in the Supporting Information).[17] This suggestion is also supported by the strongly emissive properties of **2a–d** in MeOH ($\lambda_{em}=554$, 533, 555, and 556 nm; $\Phi_F=0.39$, 0.69, 0.37, and 0.41, respectively) and in CH_2Cl_2 as already described (Figures S11–S13 in the Supporting Information).

Dynamic light scattering (DLS) measurements on **2b–d** (1×10^{-5} M) in aqueous solutions suggest the formation of aggregates with averaged medium sizes at 70 °C of 209, 181, and 105 nm, respectively, whereas those at 20 °C exhibit fairly random diagrams with larger distributions (Figure S16 in the Supporting Information).[18] The stacking assemblies inferable from the spectroscopic analyses would be based on efficient overlaps at the hydrophobic core π-planes. More concentrated aqueous solutions of **2b–d** (1×10^{-4} M) show precipitation upon heating at about 36, 56, and 95 °C, respectively, as lower critical solution temperatures (LCSTs), because dehydration around PEG chains outweighs the effect of the disaggregation of molecules at higher temperatures.[16b] The variable-temperature (VT) UV/Vis absorption spectra of **2b–d** in aqueous solution might suggest irreversible transition processes between several aggregated forms on treatment at high temperature (ca. 90 °C). In addition, with use of optical waveguides, solid films cast from aqueous solutions of **2b–d** have almost the same red-shifted UV/Vis absorption profiles ($\lambda_{max}=526$, 540, and 530 nm, respectively; Figure 2) as those cast from CH_2Cl_2 solutions ($\lambda_{max}=531$, 541, and 535 nm; Figure S17 in the Supporting Information), suggesting that the removal of water molecules by slow evaporation at room temperature disrupts the H-aggregate formations and, instead, produces the J-aggregates. Furthermore, freeze-drying is also not efficient in sustaining the solid-state organized structures as observed in aqueous solution, as is suggested by the red-shifted J-like UV/Vis absorption spectra of these amphiphilic receptors (e.g., **2c**) in the solid state (film) obtained by this procedure.[19] These results from solid-state absorptions with or without freeze-drying suggest that the formation of H-aggregates in aqueous solution is supported by water molecules, and that the removal of water molecules around the assemblies results in the formation of different assembled structures (J-type aggregates; Figure 3a), as observed in the reported single-crystal X-ray structures of the receptors (e.g., **1a**;[9a] Figure 3b).

Next, the morphologies of the transformed organized structures obtained from aqueous solution were examined. Only larger assemblies without specific shapes were observed by transmission electron microscopy (TEM) analysis

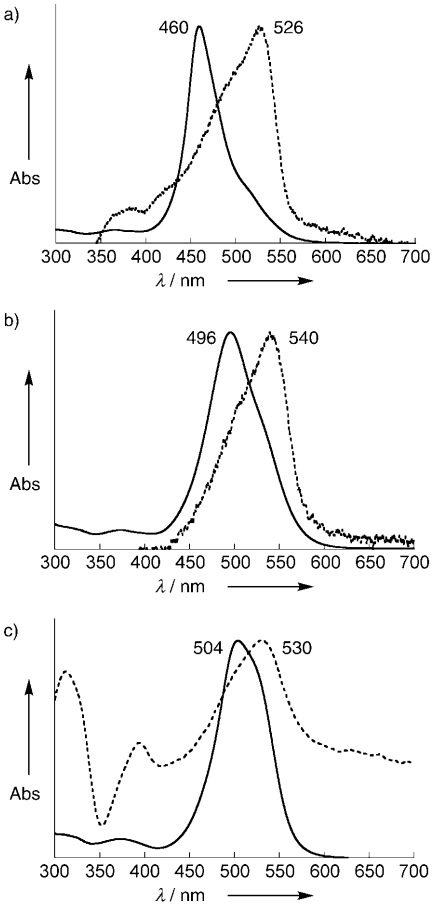

Figure 2. UV/Vis absorption spectra of a) **2b**, b) **2c**, and c) **2d** as solid-state cast from aqueous solution (-----) and in aqueous solution (——).

of aqueous solutions (1×10^{-5} M) of tetra-TEG-substituted **2b**, hexa-TEG-substituted **2c**, and hexa-HEG-substituted **2d** with $UO_2(OAc)_2$ staining (Figure S18 in the Supporting Information). In contrast, small rope-like network structures of about 5 nm in width were observed by cryogenic TEM (cryo-TEM) analysis of **2c** (1×10^{-5} M; Figure 4). In aqueous

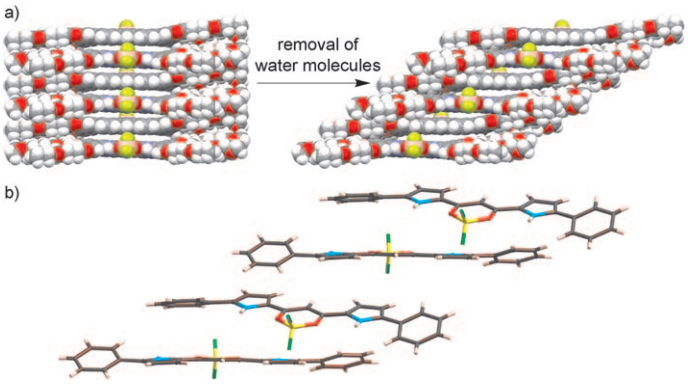

Figure 3. a) Possible proposed transition pathway (for **2c**) from H-aggregates to J-aggregates through removal of water molecules, and b) slipped stacking structures of **1a** in the solid state.[9a]

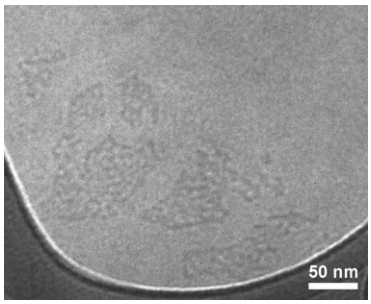

Figure 4. Cryo-TEM image of **2c** obtained from aqueous solution (1×10^{-5} M) without staining.

solution, **2c** appears to be soluble as an H-aggregated network object, possibly fabricated through π–π stacking of the core planes and interactions between the hydrophilic side chains and water molecules. The widths of 5 nm are consistent with the bundled architectures consisting of pairs of the π–π stacking columns. In this case, TEG substituents can effectively function as the hydrophilic components of the networks associating with water molecules. Removal of water molecules around the hydrophilic parts of the nanoscale networks during the preparation of conventional TEM samples might be expected to result in their assembly to form larger objects without specific morphologies through interaction between the hydrophilic side chains.

Self-assemblies of amphiphilic anion receptors with both PEG and long aliphatic chains (type B) in aqueous solution: Similarly to the self-assemblies based on **2b–d** (type A) in aqueous solution, those of **3a** and **3b** (type B) are also very fascinating. The formation of nanoarchitectures in aqueous solution was suggested by their solvent-dependent UV/Vis absorption spectra (Figure S11 in the Supporting Information). The amphiphiles **3c** and **3d**, though, are either completely insoluble or less soluble, respectively, in water, possibly due to their more hydrophobic hexadecyloxy groups. Although the solubilities of **3a–d** in aqueous solution cannot be explained in detail at this time, the lengths of the hydrophilic and hydrophobic chains appear to be essential.

The receptors **3a** and **3b** (1×10^{-5} M) exhibited absorption maxima at 462 and 481 nm, respectively, in water and at 510 and 512 nm in MeOH. These results are quite similar to those seen in the cases of **2b–d** (type A), which exist as H-aggregates in aqueous solution and as monomers in MeOH (Figure 5). The stacking interactions of **3a** and **3b** are fairly strong relative to those of the amphiphiles **2b–d** (type A), possibly due to the existence of the aliphatic long chains in the type B derivatives, as observed in the smaller proportions of water (ca. 30 and 40%), which are necessary before blue shifts are observed. Furthermore, **3a** has more tightly stacked H-aggregates than **3b**, due to the shorter hydrophilic chains in **3a**, as also observed in the cases of **2c** and **2d**. The fluorescence emissions of **3a** and **3b** in aqueous solution are observed at 672 and 671 nm (Figure S11 in the Supporting Information) with emission quantum yields (Φ_F, determined at λ_{ex} values equal to the corresponding λ_{max} values) of 0.02 and 0.02, respectively, in contrast with those in MeOH [$\Phi_F=0.32$ ($\lambda_{em}=558$ nm) for **3a** and 0.35 ($\lambda_{em}=$

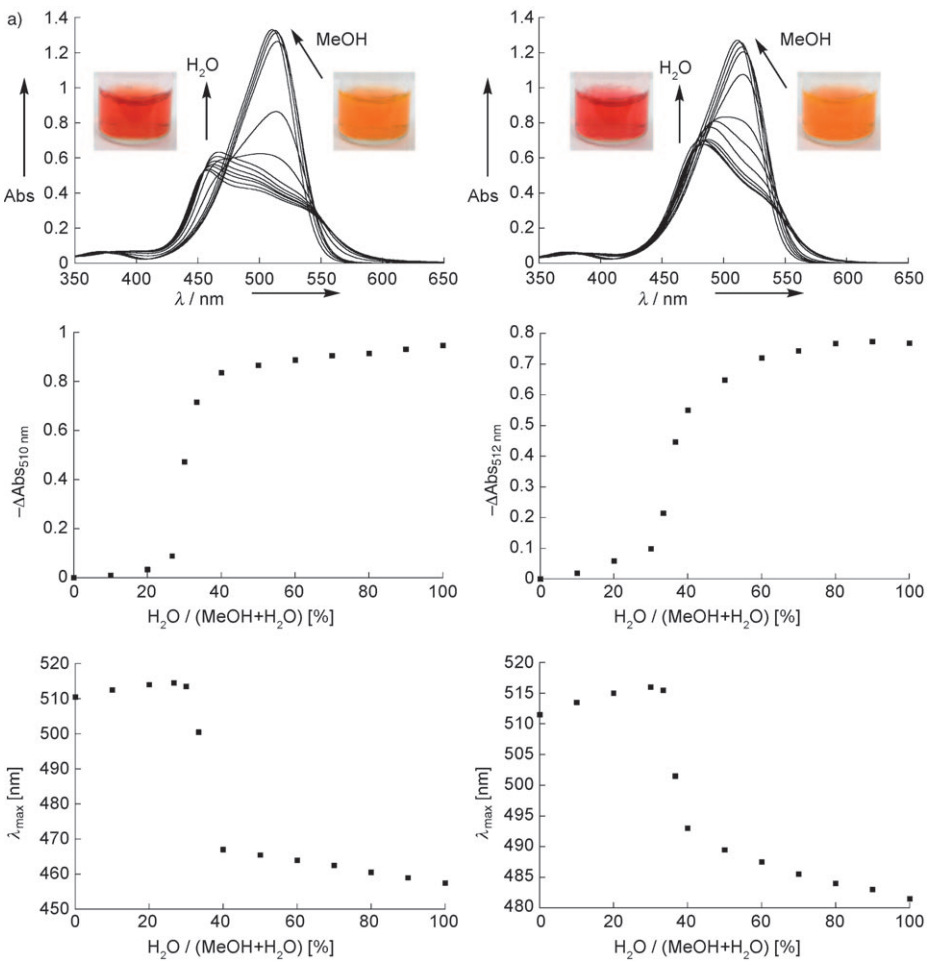

Figure 5. UV/Vis absorption spectral changes in H_2O/MeOH mixed solvents (1×10^{-5} M) and the color changes in H_2O and MeOH (insets, 5×10^{-4} M) (top), the changes in the absorbances at the λ_{max} in MeOH according to the proportion (*v*/*v*) of water (middle), and the changes in the λ_{max} values according to the proportion (*v*/*v*) of water (bottom): a) **3a**, and b) **3b**.

558 nm) for **3b**]. Red shifts in the emissions of **3a** and **3b** in aqueous solutions, unlike those of **2b–d**, originate from the aggregates and not from the monomers, as is suggested by excitation spectra, due to tighter stacking behavior of **3a** and **3b** (type B) than of **2b–d** (type A). Furthermore, DLS measurements on **3a** (1×10^{-5} M) at 70 °C exhibited aggregates with the averaged medium size of 184 nm, which is quite different from the diagrams at 20 °C, with a large distribution. In the case of **3b** (1×10^{-5} M), on the other hand, DLS analyses at 20 °C (85 nm) and at 70 °C (113 nm) appear fairly similar (Figure S16 in the Supporting Information).[18] Like those cast from **2b–d**, the solid films cast from aqueous solutions of **3a** and **3b** exhibit the formation of J-aggregates, as suggested by the UV/Vis absorption profiles ($\lambda_{max}=548$ and 531 nm, respectively, Figure 6), which are similar to those cast from CH_2Cl_2 solutions ($\lambda_{max}=543$ and 530 nm; Figure S17 in the Supporting Information).

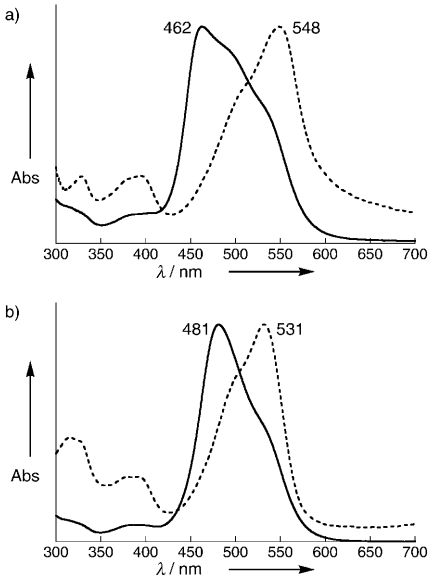

Figure 6. UV/Vis absorption spectra of a) **3a** and b) **3b** as solid-state cast from aqueous solution (-----) and in aqueous solution (——).

TEM analyses of aqueous solutions (1×10^{-5} M) of **3a** and **3b** with $UO_2(OAc)_2$ staining showed the formation of capsules of diameters in the 50–150 nm range (Figure 7a) and cylindrical aggregates, respectively, as the transformed objects formed by removal of water molecules around the hydrophilic moieties (Figure S18 in the Supporting Information). We cannot as yet confirm the extent of the effect of the assembled modes—H- and J-aggregates—on the organized structures, but some insights have been obtained for speculation on the effect of the water-assisted assembled structures. Furthermore, cryo-TEM analysis of **3a** (1×10^{-5} M) also showed vesicular structures with diameters of 30–80 nm (Figure 7b), which are consistent with the results of DLS measurements. The wall thickness (dark part) of the capsules is estimated to be about 5 nm, which suggests hydrophobic segments consisting of bilayers of amphiphilic molecules (ca. 3.9 nm by AM1 calculation). Among organized architectures, vesicles are supramolecular self-assemblies consisting of amphiphiles, such as the intracellular membrane-enclosed capsules in biotic systems.[13] In most cases, including that of biotic lipids, hydrophilic head groups face toward the aqueous phases to maintain hydrophobic tails inside the assemblies. Unlike the amphiphile **2c** (type A), possessing only hydrophilic chains, **3a** (type B) might possibly form bilayers like biotic lipids through the use of hydrophobic interactions of aliphatic chains and the location of hydrophilic TEG chains outside the layers to produce water-soluble vesicles (Figure 7c).[20]

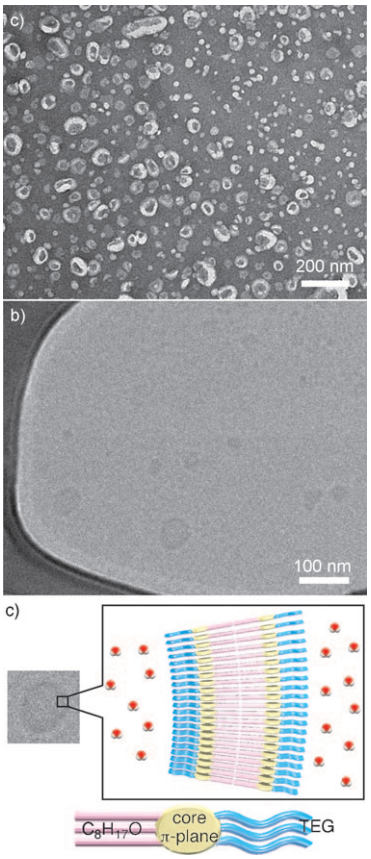

Figure 7. Images of a) TEM of **3a** from aqueous solution (1×10^{-5} M) with $UO_2(OAc)_2$ staining, and b) cryo-TEM of **3a** from aqueous solution (1×10^{-5} M) without staining. c) Possible assembling mode of **3a** in vesicles.

Self-assembly of amphiphilic anion receptors in a nonpolar solvent (hexane): Just as the amphiphiles (**2b–d**, **3a**, and **3b**) in aqueous solutions are transformed from H-aggregates into J-type assemblies on removal of solvent molecules, whereas those in CH_2Cl_2 are transformed into J-aggregates from monomers (see above), nonpolar solvents such as hexane also enhance π–π stacking interactions to produce assemblies in these solutions.[21] The UV/Vis absorption spectrum of hexa-HEG-substituted **2d**, which is almost insoluble in hexane, shows the formation of J-aggregates in the form of red-shifted absorptions ($\lambda_{max}=526$ nm), although

the other amphiphiles of type A (**2a–c**) are completely insoluble in this solvent. The type B compounds **3a–d**, on the other hand, are "soluble" in hexane (1×10^{-5} M) at 20 °C as mixtures of monomers and aggregates (Figure S19 in the Supporting Information), whereas at 60 °C they exist as monomers ($\lambda_{max}=500$, 505, 500, and 505 nm, respectively; Figure 8), like the derivative with six hexadecyloxy chains, which is soluble in octane at room temperature.[9a] Less polar hexane stabilizes the ground states of the amphiphiles to produce absorption maxima that are blue-shifted relative to those seen in CH_2Cl_2 (519–520 nm) and MeOH (510–512 nm), corresponding to monomer forms.

Upon cooling of the **3a** and **3b** solutions to −60 °C, absorptions are observed in the red-shift region, either as a shoulder (ca. 540 nm, **3a**) or as a new peak (547 nm, **3b**) (Figure 8a,b), suggesting the formation of J-aggregates as mixtures with monomers. In sharp contrast, cooling of **3c** or **3d** solutions to −60 °C results in spectral changes with blue shifts to 444 (**3c**) or 455 nm (**3d**) (Figure 8c,d), indicating the formation of H-aggregates in the case of hexadecyloxy-substituted amphiphiles. The observation of the slight red shifts (509 and 519 nm) at 20 and 40 °C in the case of **3d**, possibly due to J-aggregates, is of interest. In the cases of **3b–d**, transitions to stable forms at low temperatures dramatically occur in the regions of 20–40, 10–20, and 10–20 °C, respectively. In these cases, small amounts of H- (**3b**) and J-aggregates (**3c**, **3d**) also appear to exist and are reflected as shoulders or small bands. Furthermore, the transitions between monomers and assembled forms are also detectable by naked eye (insets of Figure 8). Such thermochromic behavior is due to temperature-responsive π–π stacking aggregation properties[22,23] of the type B amphiphiles in hexane.

The type B amphiphiles exhibit the formation of aggregates and, fascinatingly, modulate their preferable assembly modes (H and J) as functions both of temperature and of aliphatic chain length (octyloxy and hexadecyloxy) not only in aqueous solution but also in nonpolar solvents. Such observations in interactions in the apolar solvent are due to one of the unique properties of these amphiphiles: their possession of both hydrophilic and hydrophobic (sp^3) chains attached to the core hydrophobic (sp^2) plane as reported here. Detailed investigations, including those of solvent effects, are important topics for future research.

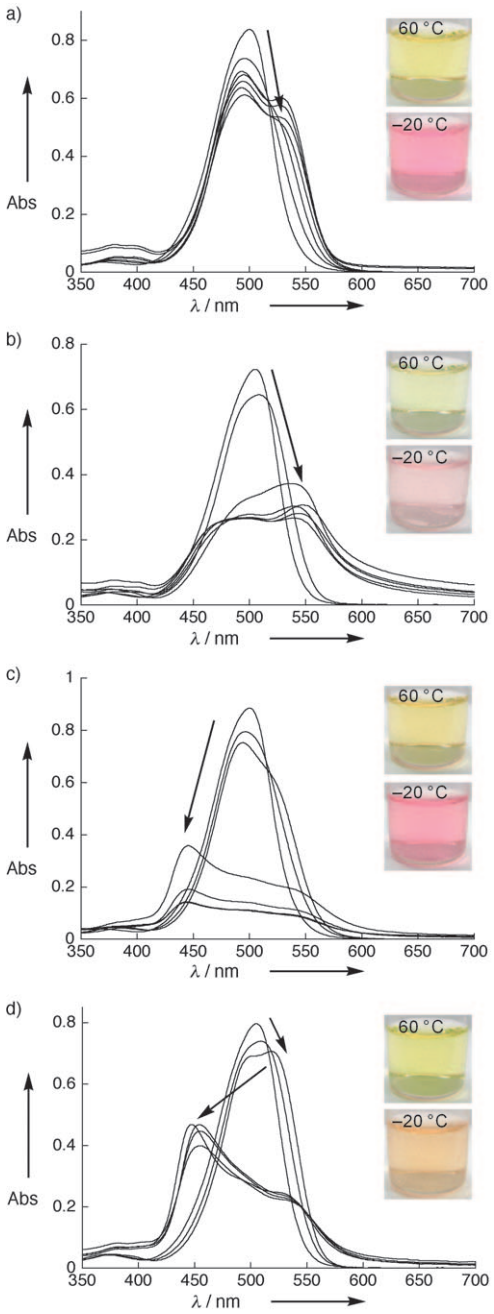

Figure 8. Variable-temperature UV/Vis absorption spectra of a) **3a**, b) **3b**, c) **3c**, and d) **3d** in hexane (1×10^{-5} M) from 60 to −60 °C in steps of 20 °C, as indicated by arrows, together with photographs at 60 and −20 °C (insets).

Sustainable behavior of the assemblies consisting of amphiphilic receptors for anions: The anion-binding behavior of the amphiphiles in aqueous solution[24] was investigated by observation of the UV/Vis absorption spectral changes of mixtures of 1, 10, and 1000 equiv of anions (F^-, Cl^-, Br^-, I^-, $CH_3CO_2^-$, $H_2PO_4^-$, and $H_2SO_4^-$) as their TBA salts and the amphiphiles (e.g., **2c** and **3a**, 1×10^{-5} M) in aqueous solutions, prepared in CH_2Cl_2 followed by evaporation of the solvent and addition of water (Figures S20 and S21 in the Supporting Information). The absorption maxima in aqueous solutions hardly shift, possibly due to i) lower anion affinities of *assembled* receptors in relation to those of the monomeric receptors, and ii) tight solvation of anions (and cations) by polar protic solvents. Slightly decreased absorbance may originate from the salting out of the aggregates from the solution associated with the ion pairs, rather than just the anions. Furthermore, like those in cases in the absence of anions, DLS measurements on **2b–d**, **3a**, and **3b** (1×10^{-5} M) in the presence of TBACl (1 equiv) in aqueous solutions show complicated profiles at 20 °C and fairly ordered ones, with averaged diameters of 336 (**2b**), 77 (**2c**), 186 (**2d**), 212 (**3a**), and 99 nm (**3b**), at 70 °C (Figure S22 in

the Supporting Information).[18] These observations also support the robustness of H-aggregates consisting of amphiphilic acyclic anion receptors in aqueous solution.[25]

Water-assisted rigid organized structures of amphiphilic anion receptors suggested by distributions between aqueous and organic solutions: The "water-soluble" amphiphiles **2b–d** (type A) and **3a** and **3b** (type B) exhibit unique behavior during the extraction processes. The amphiphiles **2b–d** (type A) are spontaneously soluble in aqueous solution, whereas **3a** and **3b** (type B) are stable as precipitates in water and become soluble upon shaking (left-hand pictures in Figure 9a–e,i). In water/CH_2Cl_2 immiscible solvent systems, the "order" of preparation is essential for the formation of aggregates.[6d] As an example, the addition of CH_2Cl_2 to aqueous solutions of **2b–d** or **3a** (1×10^{-4} M) and subsequent extraction results in aqueous upper phases containing larger quantities of amphiphiles than the organic lower phases (Figure 9a–d,i). The "structures" in both layers are postulated from the UV/Vis absorption spectra in each phase under diluted conditions (1×10^{-5} M). The spectra of the amphiphiles (e.g., **2c** and **3a**) in the CH_2Cl_2 phases are quite similar to those in the pure solutions (as monomers), whereas those in the aqueous phases correspond to mixtures of H- and J-type aggregates, suggesting that the CH_2Cl_2-saturated aqueous solution also prefers J-like states, and not just H-aggregates, possibly due to solvation of the amphiphiles by small amounts of the less polar solvent molecules (Figure S23 in the Supporting Information). DLS measurements on the amphiphiles in the aqueous phases showed the formation of fairly ordered assemblies, relative to those in ordinary aqueous solutions, with discrete medium sizes both at 20 and at 70 °C (Figure S24 in the Supporting Information).[26] This result may suggest that only "non-standard" assemblies, as well as small amounts of monomers, can be readily extracted into the organic (CH_2Cl_2) phase, due to their lower tendency to stay in the hydrophilic environments. Furthermore, and in sharp contrast, amphiphiles **2b–d** and **3a**, existing as their monomeric forms, in CH_2Cl_2 solution cannot be extracted into an aqueous phase (Figure 9a–d,ii). These observations suggest that, once formed in aqueous solution, the self-assemblies are stable and resist extraction into an organic phase (CH_2Cl_2).[27]

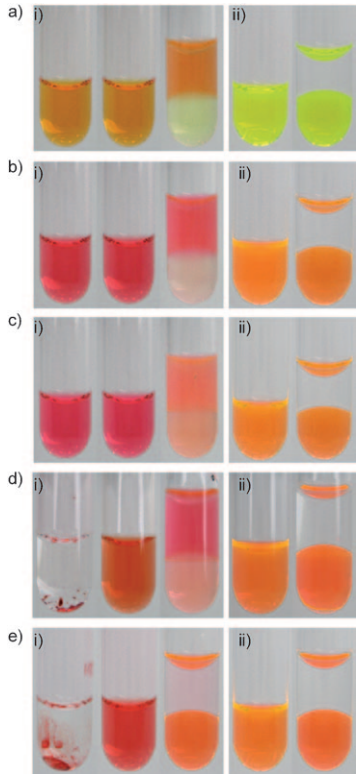

Figure 9. Photographs of extraction processes of a) **2b**, b) **2c**, c) **2d**, d) **3a**, and e) **3b**: i) aqueous solutions before shaking (left), two phases (water and CH_2Cl_2; right), and extraction from the aqueous solutions (center); ii) two phases (water and CH_2Cl_2; right), and extraction from the CH_2Cl_2 solutions (left). Initial concentrations are 1×10^{-4} M.

Unlike **2b–d** and **3a**, the amphiphile **3b** undergoes almost complete extraction with CH_2Cl_2 (Figure 9e,i), whereas, as in the cases of the other amphiphiles, water cannot extract **3b** from a CH_2Cl_2 solution (Figure 9e,ii). As shown in Figure 5, **3b** forms less stable stacking assemblies than **3a**, so the organized structures of **3b** in an aqueous solution should be readily extracted into a CH_2Cl_2 phase, even though **3b** has longer hydrophilic chains. The metastable situations for the distributions between two immiscible solvents (water and CH_2Cl_2 in this case) are found to depend on the substituents of the molecules and the stability of each assembly in aqueous solution. Furthermore, the initial conditions, based on water-assisted aggregation and CH_2Cl_2-supported disaggregation, are crucial in providing the desired metastable states in the different solvent systems.

Conclusions

In this article we have reported the synthesis of anion-responsive amphiphiles that form solvent-assisted organized structures. From observations such as the binding affinity toward anions and extraction experiments performed with an immiscible organic solvent, it has been observed that the π-conjugated acyclic oligopyrroles based on 1,3-dipyrrolylpropane-1,3-dione units, in which the π components are connected by single bonds, enter into more rigid π–π stacking interactions than expected; the H-type assemblies in aqueous solutions form nanoscale networks and vesicular structures detectable by cryo-TEM. The H-aggregates are sensitive to the conditions and are transformed into J-aggregates on removal of water. Formation mechanisms and styles of nanoscale structures such as vesicles depend on the molecular structures of the building amphiphiles. Therefore, modifications in the numbers, positions, and shapes of the peripheral substituents should result in versatile, unique organized architectures and stimuli-responsive soft materials with various potential utilities such as carrier and exciton mobility. In

addition, even though further efforts are required in order to predict the exact assembled modes by theoretical studies, due to the less symmetrical structures of the amphiphiles, it is crucial to elucidate the factors and mechanism of assembly formation in detail. This is currently being investigated.

Experimental Section

Starting materials were purchased from Wako Chemical Co., Nacalai Chemical Co., and Aldrich Chemical Co. and were used without further purification unless otherwise stated. Aqueous solutions of the amphiphiles for various analyses were prepared from water of spectroscopic grade (Wako). UV/Vis spectra were recorded with a Hitachi U-3500 spectrometer for the solution state and with a System Instruments SIS-50 surface and interface spectrometer for the solid state. Variable-temperature UV/Vis spectra were obtained with the aid of a Unisoku USP-203 A spectrophotometer cryostat. Fluorescence spectra and quantum yields were recorded with a Hitachi F-4500 fluorescence spectrometer for ordinary solutions and a Hamamatsu C9920-02 quantum yield measurement system for organic LED materials. NMR spectra used in the characterization of products were recorded on a JEOL ECA-600 600 MHz spectrometer. All NMR spectra were referenced to solvent. Fast atom bombardment mass spectrometric studies (FAB-MS) were performed with a JEOL-GCmate instrument in the positive ion mode with a 3-nitrobenzyl alcohol matrix. Electrospray ionization mass spectrometric studies (ESI-MS) were recorded with a BRUKER microTOF instrument by negative mode ESI-TOF. TLC analyses were carried out on aluminum sheets coated with silica gel 60 (Merck 5554). Column chromatography was performed on Sumitomo alumina KCG-1525, Wakogel C-300, and Merck silica gel 60 and 60 H.

4-Bromo-1-TEG-benzene: Pulverized K_2CO_3 (880.2 mg, 6.4 mmol) was added to a DMF (9 mL) solution of 4-bromophenol (732.5 mg, 4.2 mmol) and triethyleneglycol (TEG) toluene-4-sulfonate (677.3 mg, 2.1 mmol), and the mixture was stirred under nitrogen at 50 °C for 27 h. The mixture was allowed to cool and poured into a separating funnel together with water (30 mL). The aqueous solution was extracted with CH_2Cl_2. The combined extracts were washed with aq. NaOH (10 %) and water. The CH_2Cl_2 layer was dried over anhydrous $MgSO_4$ and concentrated to give an oil. The residue was then chromatographed over silica gel (Wakogel C-300, 1 % MeOH/CH_2Cl_2) to give 4-bromo-1-TEG-benzene (583.3 mg, 86 %) as a colorless oil. R_f = 0.63 (EtOAc); ^{1}H NMR (600 MHz, $CDCl_3$, 20 °C): δ = 7.36 (m, 2 H; Ar-H), 6.80 (m, 2 H; Ar-H), 4.09 (m, 2 H; OCH_2), 3.85 (m, 2 H; OCH_2), 3.73 (m, 2 H; OCH_2), 3.68 (m, 2 H; OCH_2), 3.65 (m, 2 H; OCH_2), 3.55 (m, 2 H; OCH_2), 3.38 ppm (s, 3 H; OCH_3); FAB-MS: *m*/*z* (%): calcd for $C_{13}H_{19}BrO_4$: 318.05 $[M]^+$; found: 318.1 (70), 319.1 (100).

5-Bromo-1,3-bis-TEG-benzene: Pulverized K_2CO_3 (542.3 mg, 3.9 mmol) was added to a DMF (8 mL) solution of 5-bromo-1,3-dihydroxybenzene[28] (221.5 mg, 1.2 mmol) and triethyleneglycol (TEG) toluene-4-sulfonate (747.0 mg, 2.4 mmol), and the system was stirred under nitrogen at 50 °C for 32 h. The mixture was allowed to cool and poured into a separating funnel together with water (10 mL), and the aqueous solution was extracted with CH_2Cl_2. The combined extracts were washed with aq. NaOH (10 %) and water. The CH_2Cl_2 layer was dried over anhydrous $MgSO_4$ and concentrated to give an oil. The residue was then chromatographed over silica gel (Wakogel C-300, 2 % MeOH/CH_2Cl_2) to give 5-bromo-1,3-bis-TEG-benzene (418.8 mg, 74 %) as a colorless oil. R_f = 0.33 (EtOAc); ^{1}H NMR (600 MHz, $CDCl_3$, 20 °C): δ = 6.67 (m, 2 H; Ar-H), 6.42 (m, 1 H; Ar-H), 4.08–3.47 (m, 24 H; OCH_2), 3.38 ppm (s, 6 H; OCH_3); FAB-MS: *m*/*z* (%): calcd for $C_{20}H_{33}BrO_8$: 480.14 $[M]^+$; found: 480.2 (19), 481.2 (100).

5-Bromo-1,2,3-tris-TEG-benzene: Pulverized K_2CO_3 (2.30 g, 16.7 mmol) was added to a DMF solution (18 mL) of 5-bromo-1,2,3-trihydroxybenzene[29] (600.5 mg, 2.9 mmol) and triethyleneglycol (TEG) toluene-4-sulfonate (3.21 g, 10.1 mmol), and the system was stirred under nitrogen at 50 °C for 33 h. The mixture was allowed to cool and poured into a separating funnel together with water (25 mL), and the aqueous solution was extracted with CH_2Cl_2. The combined extracts were dried over anhydrous $MgSO_4$, and DMF was removed in vacuo to give an oil. The residue was then chromatographed over silica gel (Wakogel C-300, 2.5 % MeOH/CH_2Cl_2) to give 5-bromo-1,2,3-tris-TEG-benzene (1.30 g, 69 %) as a colorless oil. R_f = 0.34 (5 % MeOH/CH_2Cl_2); ^{1}H NMR (600 MHz, $CDCl_3$, 20 °C): δ = 6.73 (s, 2 H; Ar-H), 4.13–3.53 (m, 36 H; OCH_2), 3.38 ppm (m, 9 H; OCH_3); FAB-MS: *m*/*z* (%): calcd for $C_{27}H_{47}BrO_{12}$: 642.23 $[M]^+$; found: 642.3 (100), 643.3 (59).

5-Bromo-1,2,3-tris-HEG-benzene: Pulverized K_2CO_3 (1.56 g, 11.2 mmol) was added to a DMF solution (18 mL) of 5-bromo-1,2,3-trihydroxybenzene (459.5 mg, 2.2 mmol) and hexaethyleneglycol (HEG) toluene-4-sulfonate (3.32 g, 7.4 mmol), and the system was stirred under nitrogen at 50 °C for 30 h. The mixture was allowed to cool and poured into a separating funnel together with water (20 mL), and the aqueous solution was extracted with CH_2Cl_2. The combined extracts were dried over anhydrous $MgSO_4$, and DMF was removed in vacuo to give an oil. The residue was then chromatographed over silica gel (Wakogel C-300, 5 % MeOH/CH_2Cl_2) to give 5-bromo-1,2,3-tris-HEG-benzene (1.78 g, 77 %) as a colorless oil. R_f = 0.41 (10 % MeOH/CH_2Cl_2); ^{1}H NMR (600 MHz, $CDCl_3$, 20 °C): δ = 6.73 (s, 2 H; Ar-H), 4.12 (m, 4 H; OCH_2), 4.10 (m, 2 H; OCH_2), 3.83 (m, 4 H; OCH_2), 3.76 (m, 2 H; OCH_2), 3.71–3.63 (m, 54 H; OCH_2), 3.55 (m, 6 H; OCH_2), 3.38 ppm (m, 9 H; OCH_3); FAB-MS: *m*/*z* (%): calcd for $C_{45}H_{83}BrO_{21}$: 1038.46 $[M]^+$; found: 1038.5 (100).

1-*tert*-Butoxycarbonyl-2-(4-TEG-phenyl)pyrrole and 2-(4-TEG-phenyl)-pyrrole: A solution of Na_2CO_3 (267.0 mg, 2.5 mmol) in water (2 mL) was added at room temperature under nitrogen to a solution of 4-bromo-1-TEG-benzene (191.1 mg, 0.60 mmol), 1-*tert*-butoxycarbonylpyrrole-2-boronic acid (169.6 mg, 0.80 mmol), and tetrakis(triphenylphosphine)palladium(0) (35.5 mg, 0.031 mmol) in 1,2-dimethoxyethane (17 mL).[30] The mixture was heated at reflux for 6 h, allowed to cool, and then partitioned between water and CH_2Cl_2. The combined extracts were dried over anhydrous $MgSO_4$ and concentrated to give an oil. The residue was then chromatographed over silica gel (Wakogel C-300, 40 % EtOAc/hexane) to give 1-*tert*-butoxycarbonyl-2-(4-TEG-phenyl)pyrrole (197.7 mg, 81 %) as a colorless oil. R_f = 0.45 (50 % EtOAc/hexane); ^{1}H NMR (600 MHz, $CDCl_3$, 20 °C): δ = 7.31 (m, 1 H; pyrrole-H), 7.25 (d, *J* = 8.4 Hz, 2 H; Ar-H), 6.89 (d, *J* = 8.4 Hz, 2 H; Ar-H), 6.20 (m, 1 H; pyrrole-H), 6.12 (m, 1 H; pyrrole-H), 4.15–3.55 (m, 12 H; OCH_2), 3.38 (s, 3 H; OCH_3), 1.38 ppm (s, 9 H; Boc); FAB-MS: *m*/*z* (%): calcd for $C_{22}H_{31}NO_6$: 405.22 $[M]^+$; found: 405.3 $[M]^+$ (100), 406.3 $[M+1]^+$ (51). The product 1-*tert*-butoxycarbonyl-2-(4-TEG-phenyl)pyrrole (197.7 mg, 0.49 mmol) was heated at reflux (160 °C) for 30 min and then allowed to cool. The residue was then chromatographed over silica gel (Wakogel C-300, 55 % EtOAc/hexane) to give 2-(4-TEG-phenyl)pyrrole as a colorless oil (105.3 mg, 71 %). R_f = 0.21 (50 % EtOAc/hexane); ^{1}H NMR (600 MHz, $CDCl_3$, 20 °C): δ = 8.34 (br, 1 H; NH), 7.38 (d, *J* = 7.8 Hz, 2 H; Ar-H), 6.93 (d, *J* = 8.4 Hz, 2 H; Ar-H), 6.83 (m, 1 H; pyrrole-H), 6.40 (m, 1 H; pyrrole-H), 6.27 (m, 1 H; pyrrole-H), 4.15 (t, *J* = 4.8 Hz, 2 H; OCH_2), 3.87 (t, *J* = 4.8 Hz, 2 H; OCH_2), 3.75 (t, *J* = 4.8 Hz, 2 H; OCH_2), 3.69 (t, *J* = 4.8 Hz, 2 H; OCH_2), 3.66 (t, *J* = 4.8 Hz, 2 H; OCH_2), 3.55 (t, *J* = 4.8 Hz, 2 H; OCH_2), 3.38 ppm (s, 3 H; OCH_3); FAB-MS: *m*/*z* (%): calcd for $C_{17}H_{23}NO_4$: 305.16 $[M]^+$; found: 305.2 (100), 306.2 (68).

1-*tert*-Butoxycarbonyl-2-(3,5-bis-TEG-phenyl)pyrrole and 2-(3,5-bis-TEG-phenyl)pyrrole: A solution of Na_2CO_3 (589.1 mg, 5.6 mmol) in water (3 mL) was added under nitrogen at room temperature to a solution of 4-bromo-1,3-bis-TEG-benzene (418.8 mg, 0.87 mmol), 1-*tert*-butoxycarbonylpyrrole-2-boronic acid (371.1 mg, 1.76 mmol), and tetrakis-(triphenylphosphine)palladium(0) (77.0 mg, 0.067 mmol) in 1,2-dimethoxyethane (35 mL). The mixture was heated at reflux for 6 h, allowed to cool, and then partitioned between water and CH_2Cl_2. The combined extracts were dried over anhydrous $MgSO_4$ and concentrated to give an oil. The residue was then chromatographed over silica gel (Wakogel C-300, 2 % MeOH/CH_2Cl_2) to give 1-*tert*-butoxycarbonyl-2-(3,5-bis-TEG-phenyl)pyrrole (475.1 mg, 64 %) as a colorless oil. R_f = 0.50 (5 % MeOH/CH_2Cl_2); ^{1}H NMR (600 MHz, $CDCl_3$, 20 °C): δ = 7.31 (m, 1 H; pyrrole-H), 6.50 (m, 2 H; Ar-H), 6.45 (m, 1 H; Ar-H), 6.20 (m, 1 H; pyrrole-H),

6.17 (m, 1H; pyrrole-H), 4.11–3.54 (m, 24H; OCH_2), 3.38 (s, 6H; OCH_3), 1.38 ppm (s, 9H; Boc); FAB-MS: *m/z* (%): calcd for $C_{29}H_{45}NO_{10}$: 567.30 $[M]^+$; found: 567.4 (100), 568.4 (86). The product 1-*tert*-butoxycarbonyl-2-(3,5-bis-TEG-phenyl)pyrrole (475.1 mg, 0.84 mmol) was heated at 160°C for 30 min and then allowed to cool. The residue was then chromatographed over silica gel (Wakogel C-300, 2% MeOH/CH_2Cl_2) to give 2-(3,5-bis-TEG-phenyl)pyrrole as a colorless oil (359.6 mg, 92%). R_f = 0.45 (5% MeOH/CH_2Cl_2); ^{1}H NMR (600 MHz, $CDCl_3$, 20°C): δ = 8.69 (br, 1H; NH), 6.84 (m, 1H; pyrrole-H), 6.68 (m, 2H; Ar-H), 6.49 (m, 1H; pyrrole-H), 6.35 (m, 1H; Ar-H), 6.27 (m, 1H; pyrrole-H), 4.15–3.55 (m, 24H; OCH_2), 3.38 ppm (s, 6H; OCH_3); FAB-MS: *m/z* (%): calcd for $C_{24}H_{37}NO_8$: 467.25 $[M]^+$; found: 467.3 (73), 468.3 (100).

1-*tert*-Butoxycarbonyl-2-(3,4,5-tris-TEG-phenyl)pyrrole and 2-(3,4,5-tris-TEG-phenyl)pyrrole: A solution of Na_2CO_3 (260.8 mg, 2.5 mmol) in water (2 mL) was added at room temperature under nitrogen to a solution of 5-bromo-1,2,3-tris-TEG-benzene (374.5 mg, 0.58 mmol), 1-*tert*-butoxycarbonylpyrrole-2-boronic acid (164.9 mg, 0.78 mmol), and tetrakis-(triphenylphosphine)palladium(0) (40.6 mg, 0.035 mmol) in 1,2-dimethoxyethane (15 mL). The mixture was heated at reflux for 6 h, allowed to cool, and then partitioned between water and CH_2Cl_2. The combined extracts were dried over anhydrous $MgSO_4$ and concentrated to give an oil. The residue was then chromatographed over silica gel (Wakogel C-300, 2.5% MeOH/CH_2Cl_2) to give 1-*tert*-butoxycarbonyl-2-(3,4,5-tris-TEG-phenyl)pyrrole (370.0 mg, 87%) as a colorless oil. R_f = 0.35 (5% MeOH/CH_2Cl_2); ^{1}H NMR (600 MHz, $CDCl_3$, 20°C): δ = 7.31 (m, 1H; pyrrole-H), 6.56 (s, 2H; Ar-H), 6.20 (m, 1H; pyrrole-H), 6.14 (m, 1H; pyrrole-H), 4.16–3.53 (m, 36H; OCH_2), 3.38 (s, 3H; OCH_3), 3.37 (s, 6H; OCH_3), 1.36 ppm (s, 9H; Boc); FAB-MS: *m/z* (%): calcd for $C_{16}H_{19}NO_2$: 729.39 $[M]^+$; found: 729.4 (100). The product 1-*tert*-butoxycarbonyl-2-(3,4,5-tris-TEG-phenyl)pyrrole (444.3 mg, 0.61 mmol) was heated at reflux (160°C) for 30 min and then allowed to cool. The residue was then chromatographed over silica gel (Wakogel C-300, 2.7% MeOH/CH_2Cl_2) to give 2-(3,4,5-tris-TEG-phenyl)pyrrole as a colorless oil (340.3 mg, 89%). R_f = 0.27 (5% MeOH/CH_2Cl_2); ^{1}H NMR (600 MHz, $CDCl_3$, 20°C): δ = 9.04 (br, 1H; NH), 6.83 (m, 1H; pyrrole-H), 6.82 (s, 2H; Ar-H), 6.41 (m, 1H; pyrrole-H), 6.25 (m, 1H; pyrrole-H), 4.23–3.54 (m, 36H; OCH_2), 3.37 (s, 3H; OCH_3), 3.37 (s, 6H; OCH_3); FAB-MS: *m/z* (%): calcd for $C_{31}H_{51}NO_{12}$: 629.34 $[M]^+$; found: 629.4 (100), 630.3 (56).

1-*tert*-Butoxycarbonyl-2-(3,4,5-tris-HEG-phenyl)pyrrole and 2-(3,4,5-tris-HEG-phenyl)pyrrole: A solution of Na_2CO_3 (585.6 mg, 5.5 mmol) in water (3 mL) was added at room temperature under nitrogen to a solution of 5-bromo-1,2,3-tris-HEG-benzene (1.760 g, 1.69 mmol), 1-*tert*-butoxycarbonylpyrrole-2-boronic acid (473.9 mg, 2.25 mmol), and tetrakis-(triphenylphosphine)palladium(0) (88.0 mg, 0.076 mmol) in 1,2-dimethoxyethane (35 mL). The mixture was heated at reflux for 4.5 h, allowed to cool, and then partitioned between water and CH_2Cl_2. The combined extracts were dried over anhydrous $MgSO_4$ and concentrated to give an oil. The residue was then chromatographed over silica gel (Wakogel C-300, 5% MeOH/CH_2Cl_2) to give 1-*tert*-butoxycarbonyl-2-(3,4,5-tris-HEG-phenyl)pyrrole (1.548 g, 81%) as a colorless oil. R_f = 0.46 (10% MeOH/CH_2Cl_2); ^{1}H NMR (600 MHz, $CDCl_3$, 20°C): δ = 7.31 (m, 1H; pyrrole-H), 6.56 (s, 2H; Ar-H), 6.20 (m, 1H; pyrrole-H), 6.14 (m, 1H; pyrrole-H), 4.13–4.15 (m, 6H; OCH_2), 3.84 (m, 4H; OCH_2), 3.79 (m, 2H; OCH_2), 3.73–3.70 (m, 6H; OCH_2), 3.67–3.63 (m, 6H; OCH_2), 3.55–3.54 (m, 6H; OCH_2), 3.38 (s, 3H; OCH_3), 3.37 (s, 6H; OCH_3), 1.36 ppm (s, 9H; Boc); FAB-MS: *m/z* (%): calcd for $C_{54}H_{95}NO_{23}$: 1125.63 $[M]^+$; found: 1125.6 (100), 1126.5 (74). The product 1-*tert*-butoxycarbonyl-2-(3,4,5-tris-HEG-phenyl)pyrrole (1.55 g, 1.37 mmol) was heated at 160°C for 20 min and then allowed to cool. The residue was then chromatographed over silica gel (Wakogel C-300, 6% MeOH/CH_2Cl_2) to give 2-(3,4,5-tris-HEG-phenyl)pyrrole as a colorless oil (1310.3 mg, 93%). R_f = 0.37 (10% MeOH/CH_2Cl_2); ^{1}H NMR (600 MHz, $CDCl_3$, 20°C): δ = 9.37 (br, 1H; NH), 6.85 (s, 2H; Ar-H), 6.82 (m, 1H; pyrrole-H), 6.40 (m, 1H; pyrrole-H), 6.23 (m, 1H; pyrrole-H), 4.23 (m, 4H; OCH_2), 4.16 (m, 2H; OCH_2), 3.83 (m, 4H; OCH_2), 3.79 (m, 2H; OCH_2), 3.72–3.61 (m, 54H; OCH_2), 3.54–3.52 (m, 6H; OCH_2), 3.37 (s, 3H; OCH_3), 3.36 ppm (s, 6H; OCH_3); FAB-MS: *m/z* (%): calcd for $C_{49}H_{87}NO_{21}$: 1025.58 $[M]^+$; found: 1025.7 (100), 1026.8 (76).

1,3-Bis[5-(4-TEG-phenyl)pyrrol-2-yl]propane-1,3-dione (2a′): In analogy to a literature procedure, a CH_2Cl_2 solution (2 mL) of 2-(4-TEG-phenyl)-pyrrole (105.3 mg, 0.35 mmol) was treated at 0°C with malonyl chloride (24.6 mg, 0.18 mmol) and stirred for 4 h at the same temperature. After confirmation of the consumption of the starting pyrrole by TLC analysis, the mixture was washed with saturated aq. Na_2CO_3 and saturated aq. NaCl, dried over anhydrous Na_2SO_4, filtered, and concentrated to dryness. The residue was then chromatographed over silica gel (Wakogel C-300, 3.5% MeOH/CH_2Cl_2) and recrystallized from CH_2Cl_2/hexane to afford **2a′** (30.6 mg, 26%) as a pale yellow solid. R_f = 0.40 (5% MeOH/CH_2Cl_2); ^{1}H NMR (600 MHz, $CDCl_3$, 20°C; diketone **2a′** is obtained as a mixture of keto and enol tautomers in the ratio of 1:0.23): δ (keto form) = 9.45 (br, 2H; NH), 7.49 (d, J = 9.0 Hz, 4H; Ar-H), 7.13 (m, 2H; pyrrole-H), 6.96 (d, J = 9.0 Hz, 4H; Ar-H), 6.49 (m, 2H; pyrrole-H), 4.22 (s, 2H; CH_2), 4.16 (m, 4H; OCH_2), 3.87 (m, 4H; OCH_2), 3.75 (m, 4H; OCH_2), 3.69 (m, 4H; OCH_2), 3.66 (m, 4H; OCH_2), 3.55 (m, 4H; OCH_2), 3.38 ppm (s, 6H; OCH_3); δ (enol form) = 16.71 (s, 1H; OH), 9.34 (s, 2H; NH), 7.50 (m, 4H; Ar-H), 6.97 (m, 4H; Ar-H), 6.95 (m, 2H; pyrrole-H), 6.52 (m, 2H; pyrrole-H), 6.33 (s, 1H; CH), 4.18–3.54 (m, 24H; OCH_2), 3.38 ppm (s, 6H; OCH_3); FAB-MS: *m/z* (%): calcd for $C_{37}H_{46}N_2O_{10}$: 678.32 $[M]^+$; found: 678.3 (84), 679.3 (100).

1,3-Bis[5-(3,5-bis-TEG-phenyl)pyrrol-2-yl]propane-1,3-dione (2b′): A CH_2Cl_2 solution (40 mL) of 2-(3,5-bis-TEG-phenyl)pyrrole (918.1 mg, 1.96 mmol) was treated at 0°C with malonyl chloride (138.4 mg, 0.98 mmol) and stirred for 2.5 h at the same temperature. After confirmation of the consumption of the starting pyrrole by TLC analysis, the reaction mixture was chromatographed over silica gel columns (Wakogel C-300, 3% MeOH/CH_2Cl_2 and 4.5% MeOH/EtOAc) to afford **2b′** (603.4 mg, 61%) as a pale yellow oil. R_f = 0.29 (5% MeOH/CH_2Cl_2). ^{1}H NMR (600 MHz, $CDCl_3$, 20°C; diketone **2b′** is obtained as a mixture of keto and enol tautomers in the ratio of 1:0.29): δ (keto form) = 9.70 (br, 2H; NH), 7.12 (m, 2H; pyrrole-H), 6.74 (m, 4H; Ar-H), 6.54 (m, 2H; pyrrole-H), 6.47 (m, 2H; Ar-H), 4.23 (s, 2H; CH_2), 4.17–3.55 (m, 48H; OCH_2), 3.37 ppm (s, 12H; OCH_3); δ (enol form) = 16.65 (br, 1H; OH), 9.57 (s, 2H; NH), 6.94 (m, 2H; pyrrole-H), 6.76 (m, 4H; Ar-H), 6.58 (m, 2H; pyrrole-H), 6.45 (m, 2H; Ar-H), 6.36 (s, 1H; CH), 4.17–3.55 (m, 48H; OCH_2), 3.38 ppm (s, 12H; OCH_3); FAB-MS: *m/z* (%): calcd for $C_{51}H_{74}N_2O_{18}$: 1002.4932 $[M]^+$; found: 1002.4 (100).

1,3-Bis[5-(3,4,5-tris-TEG-phenyl)pyrrol-2-yl]propane-1,3-dione (2c′): A CH_2Cl_2 solution (35 mL) of 2-(3,4,5-tris-TEG-phenyl)pyrrole (1.132 g, 1.80 mmol) was treated at 0°C with malonyl chloride (126.8 mg, 0.90 mmol) and stirred for 3 h at the same temperature. After confirmation of the consumption of the starting pyrrole by TLC analysis, the reaction mixture was chromatographed over silica gel columns (Wakogel C-300, 3.6% MeOH/CH_2Cl_2 and 12% MeOH/EtOAc) to afford **2c′** (668.3 mg, 56%) as a pale yellow oil. R_f = 0.24 (5% MeOH/CH_2Cl_2); ^{1}H NMR (600 MHz, $CDCl_3$, 20°C; diketone **2c′** is obtained as a mixture of keto and enol tautomers in the ratio of 1:0.28): δ (keto form) = 9.90 (br, 2H; NH), 7.11 (m, 2H; pyrrole-H), 6.85 (s, 4H; Ar-H), 6.49 (m, 2H; pyrrole-H), 4.25–3.53 (m, 72H; OCH_2), 3.36 ppm (m, 18H; OCH_3); δ (enol form) = 16.74 (s, 1H; OH), 9.79 (br, 2H; NH), 6.95 (m, 2H; pyrrole-H), 6.88 (s, 4H; Ar-H), 6.53 (m, 2H; pyrrole-H), 6.38 (s, 1H; CH), 4.25–3.53 (m, 72H; OCH_2), 3.37 ppm (m, 18H; OCH_3); ESI-TOF-MS: *m/z* (%): calcd for $C_{65}H_{101}N_2O_{26}$: 1325.66 $[M-H]^-$; found: 1325.7 (100), 1326.7 (64).

1,3-Bis[5-(3,4,5-tris-HEG-phenyl)pyrrol-2-yl]propane-1,3-dione (2d′): A CH_2Cl_2 solution (12 mL) of 2-(3,4,5-tris-HEG-phenyl)pyrrole (640.7 mg, 0.62 mmol) was treated at 0°C with malonyl chloride (52.7 mg, 0.38 mmol) and stirred for 1.5 h at the same temperature. After confirmation of the consumption of the starting pyrrole by TLC analysis, the reaction mixture was purified by silica gel flash column chromatography (5.5% MeOH/CH_2Cl_2) over silica gel columns to afford **2d′** (158.1 mg, 24%) as a pale yellow oil. R_f = 0.37 (10% MeOH/CH_2Cl_2); ^{1}H NMR (600 MHz, $CDCl_3$, 20°C; diketone **2d′** is obtained as a mixture of keto and enol tautomers in the ratio of 1:0.45): δ (keto form) = 10.24 (br, 2H; NH), 7.10 (m, 2H; pyrrole-H), 6.91 (s, 4H; Ar-H), 6.48 (m, 2H; pyrrole-H), 4.25 (s, 2H; CH_2), 4.23–3.52 (m, 144H; OCH_2), 3.35 ppm (m, 18H; OCH_3); δ (enol form) = 10.08 (br, 2H; NH), 6.96 (m, 2H; pyrrole-H),

6.94 (s, 4H; Ar-H), 6.52 (m, 2H; pyrrole-H), 6.44 (s, 1H; CH), 4.23–3.52 (m, 144H; OCH_2), 3.36 (m, 18H; OCH_3); ESI-TOF-MS: *m/z* (%): calcd for $C_{101}H_{173}N_2O_{44}$: 2118.14 $[M-H]^-$; found: 2118.1 (93), 2119.1 (100).

1-[5-(3,4,5-Trioctyloxyphenyl)pyrrol-2-yl]-3-[5-(3,4,5-tris-TEG-phenyl)-pyrrol-2-yl]propane-1,3-dione (3a′): A CH_2Cl_2 solution (15 mL) of 2-(3,4,5-tris-TEG-phenyl)pyrrole (241.9 mg, 0.38 mmol) and 2-(3,4,5-trioctyloxyphenyl)pyrrole (201.0 mg, 0.38 mmol) was treated at room temperature with malonyl chloride (56.5 mg, 0.40 mmol) and stirred at the same temperature for 1 h. After confirmation of the consumption of the starting pyrrole by TLC analysis, the reaction mixture was chromatographed over silica gel columns (Wakogel C-300, 2.5% MeOH/CH_2Cl_2) to afford **3a′** (93.4 mg, 20%) as a pale yellow oil. R_f=0.28 (5% MeOH/CH_2Cl_2); ^{1}H NMR (600 MHz, $CDCl_3$, 20°C; diketone **3a′** is obtained as a mixture of keto and enol tautomers in the ratio of 1:0.50): δ (keto form)=9.87 (br, 1H; NH), 9.44 (br, 1H; NH), 7.12 (m, 2H; pyrrole-H), 6.85 (s, 2H; Ar-H), 6.72 (s, 2H; Ar-H), 6.49 (m, 2H; pyrrole-H), 4.25–4.17 (m, 6H; OCH_2), 4.04–3.96 (m, 6H; $OCH_2C_7H_{15}$), 3.88–3.85 (m, 4H; OCH_2), 3.81–3.79 (m, 2H; OCH_2), 3.76–3.62 (m, 18H; OCH_2), 3.56–3.53 (m, 6H; OCH_2), 3.38–3.35 (m, 9H; OCH_3), 1.86–1.72 (m, 6H; $OCH_2CH_2C_6H_{13}$), 1.50–1.47 (m, 6H; $OC_2H_4CH_2C_5H_{11}$), 1.36–1.28 (m, 24H; $OC_3H_6C_4H_8CH_3$), 0.88 ppm (m, 9H; CH_3); δ (enol form)=16.75 (s, 1H; OH), 9.76 (br, 1H; NH), 9.34 (br, 1H; NH), 6.95 (m, 2H; pyrrole-H), 6.88 (s, 2H; Ar-H), 6.74 (s, 2H; Ar-H), 6.53 (m, 2H; pyrrole-H), 6.37 (s, 1H; CH), 4.25–4.17 (m, 6H; OCH_2), 4.04–3.96 (m, 6H; $OCH_2C_7H_{15}$), 3.88–3.85 (m, 4H; OCH_2), 3.81–3.79 (m, 2H; OCH_2), 3.76–3.62 (m, 18H; OCH_2), 3.38–3.35 (m, 9H; OCH_3), 3.37 (s, 6H; OCH_3), 1.86–1.72 (m, 6H; $OCH_2CH_2C_6H_{13}$), 1.50–1.47 (m, 6H; $OC_2H_4CH_2C_5H_{11}$), 1.36–1.28 (m, 24H; $OC_3H_6C_4H_8CH_3$), 0.88 ppm (m, 9H; CH_3); ESI-TOF-MS: *m/z* (%): calcd for $C_{68}H_{107}N_2O_{17}$: 1223.76 $[M-H]^-$; found: 1223.8 (100), 1224.8 (72).

1-[5-(3,4,5-Trioctyloxyphenyl)pyrrol-2-yl]-3-[5-(3,4,5-tris-HEG-phenyl)-pyrrol-2-yl]propane-1,3-dione (3b′): A CH_2Cl_2 solution (11 mL) of 2-(3,4,5-tris-HEG-phenyl)pyrrole (279.6 mg, 0.27 mmol) and 2-(3,4,5-trioctyloxyphenyl)pyrrole (142.9 mg, 0.27 mmol) was treated at room temperature with malonyl chloride (41.7 mg, 0.30 mmol) and stirred at the same temperature for 1 h. After confirmation of the consumption of the starting pyrrole by TLC analysis, the reaction mixture was chromatographed over silica gel columns (Wakogel C-300, 4.5% MeOH/CH_2Cl_2) to afford **3b′** (129.4 mg, 29%) as a pale yellow oil. R_f=0.37 (10% MeOH/CH_2Cl_2). ^{1}H NMR (600 MHz, $CDCl_3$, 20°C; diketone **3b′** is obtained as a mixture of keto and enol tautomers in the ratio of 1:0.36): δ (keto form)=9.94 (br, 1H; NH), 9.48 (br, 1H; NH), 7.12 (m, 2H; pyrrole-H), 6.89 (s, 2H; Ar-H), 6.73 (s, 2H; Ar-H), 6.49 (m, 2H; pyrrole-H), 4.22 (s, 2H; CH_2) 4.26–4.17 (m, 6H; OCH_2), 4.04–3.88 (m, 6H; $OCH_2C_7H_{15}$), 3.86 (m, 4H; OCH_2), 3.80 (m, 2H; OCH_2), 3.73–3.61 (m, 54H; OCH_2), 3.54–3.52 (m, 6H; OCH_2), 3.36–3.35 (m, 9H; OCH_3), 1.86–1.72 (m, 6H; $OCH_2CH_2C_6H_{13}$), 1.51–1.46 (m, 6H; $OC_2H_4CH_2C_5H_{11}$), 1.38–1.25 (m, 24H; $OC_3H_6C_4H_8CH_3$), 0.90–0.87 ppm (m, 9H; CH_3); δ (enol form)=16.74 (s, 1H; OH), 9.85 (br, 1H; NH), 9.37 (br, 1H; NH), 6.96 (m, 2H; pyrrole-H), 6.92 (s, 2H; Ar-H), 6.74 (s, 2H; Ar-H), 6.53 (m, 2H; pyrrole-H), 6.40 (s, 1H; CH), 4.26–4.17 (m, 6H; OCH_2), 4.04–3.88 (m, 6H; $OCH_2C_7H_{15}$), 3.86 (m, 4H; OCH_2), 3.80 (m, 2H; OCH_2), 3.73–3.61 (m, 54H; OCH_2), 3.54–3.52 (m, 6H; OCH_2), 3.36–3.35 (m, 9H; OCH_3), 1.86–1.72 (m, 6H; $OCH_2CH_2C_6H_{13}$), 1.51–1.46 (m, 6H; $OC_2H_4CH_2C_5H_{11}$), 1.38–1.25 (m, 24H; $OC_3H_6C_4H_8CH_3$), 0.90–0.87 ppm (m, 9H; CH_3); ESI-TOF-MS: *m/z* (%): calcd for $C_{86}H_{143}N_2O_{26}$: 1619.99 $[M-H]^-$; found: 1620.0 (100), 1621.0 (96).

1-[5-(3,4,5-Trihexadecyloxyphenyl)pyrrol-2-yl]-3-[5-(3,4,5-tris-TEG-phenyl)pyrrol-2-yl]propane-1,3-dione (3c′): A CH_2Cl_2 solution (11 mL) of 2-(3,4,5-tris-TEG-phenyl)pyrrole (179.3 mg, 0.29 mmol) and 2-(3,4,5-trihexadecyloxyphenyl)pyrrole (246.3 mg, 0.29 mmol) was treated at room temperature with malonyl chloride (44.2 mg, 0.31 mmol) and stirred at the same temperature for 1 h. After confirmation of the consumption of the starting pyrrole by TLC analysis, the reaction mixture was chromatographed over silica gel columns (Wakogel C-300, 2.5% MeOH/CH_2Cl_2 and 5% MeOH/EtOAc) to afford **3c′** (120.8 mg, 27%) as a pale yellow oil. R_f=0.23 (5% MeOH/CH_2Cl_2); ^{1}H NMR (600 MHz, $CDCl_3$, 20°C; diketone **3c′** is obtained as a mixture of keto and enol tautomers in the ratio of 1:0.37): δ (keto form)=9.81 (br, 1H; NH), 9.42 (br, 1H; NH), 7.12 (m, 2H; pyrrole-H), 6.85 (s, 2H; Ar-H), 6.71 (s, 2H; Ar-H), 6.49 (m, 2H; pyrrole-H), 4.23 (s, 2H; CH_2) 4.25–4.17 (m, 6H; OCH_2), 4.04–3.95 (m, 6H; $OCH_2C_7H_{15}$), 3.87 (m, 4H; OCH_2), 3.80 (m, 2H; OCH_2), 3.76–3.62 (m, 18H; OCH_2), 3.56–3.53 (m, 6H; OCH_2), 3.38–3.35 (m, 9H; OCH_3), 1.85–1.72 (m, 6H; $OCH_2CH_2C_{14}H_{29}$), 1.50–1.45 (m, 6H; $OC_2H_4CH_2C_{13}H_{27}$), 1.38–1.25 (m, 72H; $OC_3H_6C_{12}H_{24}CH_3$), 0.88 ppm (m, 9H; CH_3); δ (enol form)=16.75 (s, 1H; OH), 9.70 (br, 1H; NH), 9.33 (br, 1H; NH), 6.95 (m, 2H; pyrrole-H), 6.87 (s, 2H; Ar-H), 6.74 (s, 2H; Ar-H), 6.53 (m, 2H; pyrrole-H), 6.37 (s, 1H; CH), 4.25–4.17 (m, 6H; OCH_2), 4.04–3.95 (m, 6H; $OCH_2C_7H_{15}$), 3.87 (m, 4H; OCH_2), 3.80 (m, 2H; OCH_2), 3.76–3.62 (m, 18H; OCH_2), 3.56–3.53 (m, 6H; OCH_2), 3.38–3.35 (m, 9H; OCH_3), 1.85–1.72 (m, 6H; $OCH_2CH_2C_{14}H_{29}$), 1.50–1.45 (m, 6H; $OC_2H_4CH_2C_{13}H_{27}$), 1.38–1.25 (m, 72H; $OC_3H_6C_{12}H_{24}CH_3$), 0.88 ppm (m, 9H; CH_3); ESI-TOF-MS: *m/z* (%): calcd for $C_{92}H_{155}N_2O_{17}$: 1560.13 $[M-H]^-$; found: 1560.1 (93), 1561.1 (100).

1-[5-(3,4,5-Trihexadecyloxyphenyl)pyrrol-2-yl]-3-[5-(3,4,5-tris-HEG-phenyl)pyrrol-2-yl]propane-1,3-dione (3d′): A CH_2Cl_2 solution (20 mL) of 2-(3,4,5-tris-TEG-phenyl)pyrrole (236.6 mg, 0.27 mmol) and 2-(3,4,5-trihexadecyloxyphenyl)pyrrole (280.6 mg, 0.27 mmol) was treated at room temperature with malonyl chloride (42.3 mg, 0.30 mmol) and stirred at the same temperature for 2 h. After confirmation of the consumption of the starting pyrrole by TLC analysis, the reaction mixture was chromatographed over silica gel flash columns (5.5% MeOH/CH_2Cl_2) to afford **3d′** (28.7 mg, 5%) as a pale yellow oil. R_f=0.30 (10% MeOH/CH_2Cl_2); ^{1}H NMR (600 MHz, $CDCl_3$, 20°C; diketone **3d′** is obtained as a mixture of keto and enol tautomers in the ratio of 1:0.35): δ (keto form)=10.18 (br, 1H; NH), 9.58 (br, 1H; NH), 7.11 (m, 2H; pyrrole-H), 6.91 (s, 2H; Ar-H), 6.74 (s, 2H; Ar-H), 6.49 (m, 2H; pyrrole-H), 4.26–4.22 (m, 4H; OCH_2), 4.19–4.17 (m, 2H; OCH_2), 4.04–3.95 (m, 6H; $OCH_2C_{15}H_{31}$), 3.88–3.85 (m, 4H; OCH_2), 3.81–3.78 (m, 2H; OCH_2), 3.74–3.61 (m, 54H; OCH_2), 3.54–3.52 (m, 6H; OCH_2), 3.36–3.35 (m, 9H; OCH_3), 1.84–1.72 (m, 6H; $OCH_2CH_2C_{14}H_{29}$), 1.50–1.45 (m, 6H; $OC_2H_4CH_2C_{13}H_{27}$), 1.38–1.25 (m, 72H; CH_2), 0.88 ppm (m, 9H; CH_3); δ (enol form)=16.70 (s, 1H; OH), 10.05 (br, 1H; NH), 9.43 (br, 1H; NH), 6.96 (m, 2H; pyrrole-H), 6.94 (s, 2H; Ar-H), 6.75 (s, 2H; Ar-H), 6.53 (m, 2H; pyrrole-H), 6.40 (s, 1H; CH), 4.26–4.22 (m, 4H; OCH_2), 4.19–4.17 (m, 2H; OCH_2), 4.04–3.95 (m, 6H; $OCH_2C_{15}H_{31}$), 3.88–3.85 (m, 4H; OCH_2), 3.81–3.78 (m, 2H; OCH_2), 3.74–3.61 (m, 54H; OCH_2), 3.54–3.52 (m, 6H; OCH_2), 3.36–3.35 (m, 9H; OCH_3), 1.84–1.72 (m, 6H; $OCH_2CH_2C_{14}H_{29}$), 1.50–1.45 (m, 6H; $OC_2H_4CH_2C_{13}H_{27}$), 1.38–1.25 (m, 72H; CH_2), 0.88 ppm (m, 9H; CH_3); ESI-TOF-MS: *m/z* (%): calcd for $C_{110}H_{191}N_2O_{26}$: 1956.37 $[M-H]^-$; found: 1956.4 (87), 1957.4 (100).

BF_2 complex of 2a′ (2a): $BF_3{\cdot}OEt_2$ (139.6 mg, 0.98 mmol) was added to a CH_2Cl_2 solution (7 mL) of diketone **2a′** (21.8 mg, 0.032 mmol), and the system was stirred at room temperature for 30 min. Silica gel column chromatography (Wakogel C-300, 2% MeOH/CH_2Cl_2) and crystallization from CH_2Cl_2/hexane afforded **2a** (10.6 mg, 45%) as a red solid. R_f=0.31 (5% MeOH/CH_2Cl_2); ^{1}H NMR (600 MHz, $CDCl_3$, 20°C): δ=9.58 (br, 2H; NH), 7.56 (m, 4H; Ar-H), 7.19 (m, 2H; pyrrole-H), 7.00 (m, 4H; Ar-H), 6.63 (m, 2H; pyrrole-H), 6.49 (s, 1H; CH), 4.20–3.56 (m, 24H; OCH_2), 3.39 ppm (s, 6H; OCH_3); UV/Vis (CH_2Cl_2): λ_{max} ($\varepsilon\times10^{-5}$)=519.0 nm (1.19 M^{-1} cm^{-1}); FAB-MS: *m/z* (%): calcd for $C_{37}H_{45}BF_2N_2O_{10}$: 726.31 $[M]^+$; found: 726.3 (100^+), 727.3 (64).

BF_2 complex of 2b′ (2b): $BF_3{\cdot}OEt_2$ (23.2 mg, 0.16 mmol) was added to a CH_2ClCH_2Cl solution (30 mL) of diketone **2b′** (108.5 mg, 0.11 mmol), and the system was stirred at reflux temperature for 15 min. The reaction mixture was first separated on a silica gel short column (Wakogel C-300, 5% MeOH/CH_2Cl_2) to eliminate acidic compounds. Purification by silica gel flash column chromatography (4.5% MeOH/CH_2Cl_2) and on an alumina short column (1% MeOH/CH_2Cl_2) then afforded **2b** (103.2 mg, 91%) as a red oil. R_f=0.47 (10% MeOH/CH_2Cl_2); ^{1}H NMR (600 MHz, $CDCl_3$, 20°C): δ=10.11 (br, 2H; NH), 7.18 (m, 2H; pyrrole-H), 6.85 (m, 4H; Ar-H), 6.67 (m, 2H; pyrrole-H), 6.52 (s, 1H; CH), 6.49 (m, 2H; Ar-H), 4.20–3.56 (m, 48H; OCH_2), 3.37 ppm (s, 12H; OCH_3); UV/Vis (CH_2Cl_2): λ_{max} ($\varepsilon\times10^{-5}$)=503.0 nm (1.22 M^{-1} cm^{-1}); FAB-MS: *m/z* (%): calcd for $C_{51}H_{73}BF_2N_2O_{18}$: 1050.49 $[M]^+$; found: 1050.5 (100), 1051.5 (88).

BF_2 complex of 2c′ (2c): BF_3·OEt_2 (167.5 mg, 1.4 mmol) was added to a CH_2Cl_2 solution (30 mL) of diketone **2c′** (123.9 mg, 0.093 mmol), and the system was stirred at 0 °C for 10 min. The reaction mixture was first separated on a silica gel short column (Wakogel C-300, 7% MeOH/CH_2Cl_2) to eliminate acidic impurities. Purification by silica gel column flash chromatography (6.5% MeOH/CH_2Cl_2) and on an alumina short column (1% MeOH/CH_2Cl_2) then afforded **2c** (63.5 mg, 49%) as a red oil. R_f = 0.37 (10% MeOH/CH_2Cl_2); ^{1}H NMR (600 MHz, $CDCl_3$, 20 °C): δ = 10.43 (br, 2H; NH), 7.19 (m, 2H; pyrrole-H), 7.01 (s, 4H; Ar-H), 6.63 (m, 2H; pyrrole-H), 6.55 (s, 1H; CH), 4.28–3.55 (m, 72H; OCH_2), 3.39 (s, 6H; OCH_3), 3.34 ppm (s, 12H; OCH_3); UV/Vis (CH_2Cl_2): λ_{max} ($\varepsilon \times 10^{-5}$) = 517.0 nm (1.16 M^{-1} cm^{-1}); FAB-MS: *m/z* (%): calcd for $C_{65}H_{101}BF_2N_2O_{26}$: 1374.67 $[M]^+$; found: 1374.7 (100).

BF_2 complex of 2d′ (2d): BF_3·OEt_2 (37.2 mg, 0.26 mmol) was added to a CH_2Cl_2 solution (7 mL) of diketone **2d′** (56.3 mg, 0.027 mmol), and the system was stirred at 0 °C for 10 min. The reaction mixture was first separated on a silica gel short column (Wakogel C-300, 6.5% MeOH/CH_2Cl_2) to eliminate acidic entities. Purification by silica gel flash column chromatography (6.5% MeOH/CH_2Cl_2) and on an alumina short column (1% MeOH/CH_2Cl_2) then afforded **2d** (26.9 mg, 51%) as a red oil. R_f = 0.35 (10% MeOH/CH_2Cl_2); ^{1}H NMR (600 MHz, $CDCl_3$, 20 °C): δ = 10.81 (br, 2H; NH), 7.21 (m, 2H; pyrrole-H), 7.09 (s, 4H; Ar-H), 6.64 (m, 2H; pyrrole-H), 6.60 (s, 1H; CH), 4.29 (m, 8H; OCH_2), 4.22 (m, 4H; OCH_2), 3.88 (m, 8H; OCH_2), 3.80 (m, 4H; OCH_2), 3.74 (m, 8H; OCH_2), 3.70–3.60 (m, 100H; OCH_2), 3.54–3.51 (m, 12H; OCH_2), 3.35 (s, 18H; OCH_3); UV/Vis (CH_2Cl_2): λ_{max} ($\varepsilon \times 10^{-4}$) = 518.0 nm (9.75 M^{-1} cm^{-1}); ESI-TOF-MS: *m/z* (%): calcd for $C_{101}H_{172}BF_2N_2O_{44}$: 2166.13 $[M-H]^-$; found: 2166.1 (100), 2167.1 (99).

BF_2 complex of 3a′ (3a): BF_3·OEt_2 (15.8 mg, 0.11 mmol) was added to a CH_2ClCH_2Cl solution (24 mL) of diketone **3a′** (90.2 mg, 0.074 mmol), and the system was stirred at reflux temperature for 10 min. The reaction mixture was first separated on a silica gel short column (Wakogel C-300, 2.5% MeOH/CH_2Cl_2) to eliminate acidic entities. Purification by silica gel flash column chromatography (2.5% MeOH/CH_2Cl_2) and on an alumina short column (1% MeOH/CH_2Cl_2) then afforded **3a** (80.5 mg, 86%) as a red oil. R_f = 0.28 (5% MeOH/CH_2Cl_2); ^{1}H NMR (600 MHz, $CDCl_3$, 20 °C): δ = 10.50 (br, 1H; NH), 9.55 (br, 1H; NH), 7.21–7.18 (m, 2H; pyrrole-H), 7.01 (s, 2H; Ar-H), 6.79 (s, 2H; Ar-H), 6.65–6.63 (m, 2H; pyrrole-H), 6.53 (s, 1H; CH), 4.27 (m, 4H; OCH_2), 4.21 (m, 2H; OCH_2), 4.06 (t, J = 6.6 Hz, 4H; $OCH_2C_7H_{15}$), 4.00 (t, J = 6.6 Hz, 2H; $OCH_2C_7H_{15}$), 3.87 (m, 4H; OCH_2), 3.80 (m, 2H; OCH_2), 3.76 (m, 4H; OCH_2), 3.70–3.57 (m, 14H; OCH_2), 3.58–3.55 (m, 6H; OCH_2), 3.39 (s, 3H; OCH_3), 3.34 (s, 6H; OCH_3), 1.86 (m, 4H; $OCH_2CH_2C_6H_{13}$), 1.76 (m, 2H; $OCH_2CH_2C_6H_{13}$), 1.54–1.47 (m, 6H; $OC_2H_4CH_2C_5H_{11}$), 1.40–1.27 (m, 24H; $OC_3H_6C_4H_8CH_3$), 0.90–0.88 ppm (m, 3H; $OC_7H_{14}CH_3$); UV/Vis (CH_2Cl_2): λ_{max} ($\varepsilon \times 10^{-5}$) = 519.0 nm (1.24 M^{-1} cm^{-1}); ESI-TOF-MS: *m/z* (%): calcd for $C_{68}H_{106}BF_2N_2O_{17}$: 1271.76 $[M-H]^-$; found: 1271.8 (100), 1272.8 (95).

BF_2 complex of 3b′ (3b): BF_3·OEt_2 (14.1 mg, 0.099 mmol) was added to a CH_2ClCH_2Cl solution (21 mL) of diketone **3b′** (107.4 mg, 0.066 mmol), and the system was stirred at reflux temperature for 10 min. The reaction mixture was first separated on a small silica gel precolumn (Wakogel C-300, 4.5% MeOH/CH_2Cl_2) to eliminate acidic entities. Purification by silica gel flash column chromatography (4.5% MeOH/CH_2Cl_2) and on an alumina short column (2% MeOH/CH_2Cl_2) then afforded **3b** (100.9 mg, 91%) as a red oil. R_f = 0.39 (10% MeOH/CH_2Cl_2); ^{1}H NMR (600 MHz, $CDCl_3$, 20 °C): δ = 10.84 (br, 1H; NH), 9.54 (br, 1H; NH), 7.22 (m, 1H; pyrrole-H), 7.19 (m, 1H; pyrrole-H), 7.12 (s, 2H; Ar-H), 6.79 (s, 2H; Ar-H), 6.65 (m, 1H; pyrrole-H), 6.63 (m, 1H; pyrrole-H), 6.57 (s, 1H; CH), 4.30 (m, 4H; OCH_2), 4.23 (m, 2H; OCH_2), 4.06 (t, J = 6.6 Hz, 4H; $OCH_2C_7H_{15}$), 4.00 (t, J = 6.6 Hz, 2H; $OCH_2C_7H_{15}$), 3.88 (m, 4H; OCH_2), 3.81 (m, 2H; OCH_2), 3.74 (m, 4H; OCH_2), 3.69–3.58 (m, 50H; OCH_2), 3.54–3.51 (m, 6H; OCH_2), 3.34 (s, 6H; OCH_3), 3.34 (s, 3H; OCH_3), 1.85 (m, 4H; $OCH_2CH_2C_6H_{13}$), 1.76 (m, 2H; $OCH_2CH_2C_6H_{13}$), 1.52–1.47 (m, 6H; $OC_2H_4CH_2C_5H_{11}$), 1.39–1.25 (m, 24H; $OC_3H_6C_4H_8CH_3$), 0.90–0.88 ppm (m, 9H; $OC_7H_{14}CH_3$); UV/Vis (CH_2Cl_2): λ_{max} ($\varepsilon \times 10^{-5}$) = 519.5 nm (1.19 M^{-1} cm^{-1}); ESI-TOF-MS: *m/z* (%): calcd for $C_{86}H_{142}BF_2N_2O_{26}$: 1667.99 $[M-H]^-$; found: 16 68.0 (100), 1669.0 (81).

BF_2 complex of 3c′ (3c): BF_3·OEt_2 (14.7 mg, 0.10 mmol) was added to a CH_2ClCH_2Cl solution (22 mL) of diketone **3c′** (106.9 mg, 0.068 mmol), and the system was stirred at reflux temperature for 10 min. The reaction mixture was first separated on a silica gel short column (Wakogel C-300, 2.5% MeOH/CH_2Cl_2) to eliminate acidic entities. Purification by silica gel flash column chromatography (2.5% MeOH/CH_2Cl_2) and on an alumina short column (1% MeOH/CH_2Cl_2) then afforded **3c** (90.0 mg, 82%) as a red solid. R_f = 0.33 (5% MeOH/CH_2Cl_2); ^{1}H NMR (600 MHz, $CDCl_3$, 20 °C): δ = 10.44 (br, 1H; NH), 9.50 (br, 1H; NH), 7.20 (m, 1H; pyrrole-H), 7.19 (m, 1H; pyrrole-H), 7.01 (s, 2H; Ar-H), 6.78 (s, 2H; Ar-H), 6.65–6.63 (m, 2H; pyrrole-H), 6.53 (s, 1H; CH), 4.27 (m, 4H; OCH_2), 4.21 (m, 2H; OCH_2), 4.06 (t, J = 6.6 Hz, 4H; $OCH_2C_{15}H_{31}$), 4.00 (t, J = 6.6 Hz, 2H; $OCH_2C_{15}H_{31}$), 3.88 (t, J = 4.8 Hz, 4H; OCH_2), 3.81 (t, J = 4.8 Hz, 2H; OCH_2), 3.76 (m, 4H; OCH_2), 3.72–3.68 (m, 10H; OCH_2), 3.63 (m, 4H; OCH_2), 3.59–3.55 (m, 6H; OCH_2), 3.40 (s, 3H; OCH_3), 3.35 (s, 6H; OCH_3), 1.85 (m, 4H; $OCH_2CH_2C_{14}H_{29}$), 1.76 (m, 2H; $OCH_2CH_2C_{14}H_{29}$), 1.53–1.46 (m, 6H; $OC_2H_4CH_2C_{13}H_{27}$), 1.40–1.26 (m, 72H; $OC_3H_6C_{12}H_{24}CH_3$), 0.89–0.86 ppm (m, 9H; $OC_{15}H_{30}CH_3$); UV/Vis (CH_2Cl_2): λ_{max} ($\varepsilon \times 10^{-5}$) = 519.0 nm (1.28 M^{-1} cm^{-1}); ESI-TOF-MS: *m/z* (%): calcd for $C_{92}H_{154}BF_2N_2O_{17}$: 1608.13 $[M-H]^-$; found: 1608.1 (100), 1609.1 (62).

BF_2 complex of 3d′ (3d): BF_3·OEt_2 (3.2 mg, 0.022 mmol) was added to a CH_2ClCH_2Cl solution (5 mL) of diketone **3d′** (28.7 mg, 0.015 mmol), and the system was stirred at reflux temperature for 10 min. The reaction mixture was first separated on a silica gel short column (Wakogel C-300, 5% MeOH/CH_2Cl_2) to eliminate acidic entities. Purification by silica gel flash column chromatography (4.5% MeOH/CH_2Cl_2) and on an alumina short column (1% MeOH/CH_2Cl_2) then afforded **3d** (20.1 mg, 68%) as a red oil. R_f = 0.39 (10% MeOH/CH_2Cl_2); ^{1}H NMR (600 MHz, $CDCl_3$, 20 °C): δ = 10.88 (br, 1H; NH), 9.58 (br, 1H; NH), 7.22 (m, 1H; pyrrole-H), 7.19 (m, 1H; pyrrole-H), 7.11 (s, 2H; Ar-H), 6.79 (s, 2H; Ar-H), 6.65 (m, 1H; pyrrole-H), 6.63 (m, 1H; pyrrole-H), 6.57 (s, 1H; CH), 4.29 (m, 4H; OCH_2), 4.22 (m, 2H; OCH_2), 4.06 (t, J = 6.6 Hz, 4H; $OCH_2C_{15}H_{31}$), 3.98 (t, J = 6.6 Hz, 2H; $OCH_2C_{15}H_{31}$), 3.88 (m, 4H; OCH_2), 3.80 (m, 2H; OCH_2), 3.73 (m, 4H; OCH_2), 3.70–3.57 (m, 50H; OCH_2), 3.53–3.51 (m, 6H; OCH_2), 3.34 (s, 9H; OCH_3), 1.85 (m, 4H; $OCH_2CH_2C_{14}H_{29}$), 1.76 (m, 2H; $OCH_2CH_2C_{14}H_{29}$), 1.53–1.46 (m, 6H; $OC_2H_4CH_2C_{13}H_{27}$), 1.39–1.25 (m, 72H; $OC_3H_6C_{12}H_{24}CH_3$), 0.89–0.86 ppm (m, 3H; $OC_{15}H_{30}CH_3$); UV/Vis (CH_2Cl_2): λ_{max} ($\varepsilon \times 10^{-5}$) = 519.0 nm (1.18 M^{-1} cm^{-1}); ESI-TOF-MS: *m/z* (%): calcd for $C_{110}H_{190}BF_2N_2O_{26}$: 2004.37 $[M-H]^-$; found: 2004.4 (81), 2005.4 (100).

Methods for DLS: DLS measurements were obtained with a Malvern Zetasizer Nano-ZS differential light scattering instrument.

Cryogenic transmission electron microscopy (cryo-TEM): The cryogenic transmission electron microscopy (cryo-TEM) experiments were performed with thin films of aqueous solutions of amphiphilic molecule (5 μL) transferred to a lacey supported grid. The thin aqueous films were prepared under controlled temperature and humidity conditions (97–99%) in a custom-built environmental chamber in order to prevent evaporation of water from sample solutions. Excess liquid was blotted with filter paper (2–3 s), and the thin aqueous films were rapidly vitrified by plunging them into liquid ethane (cooled by liquid nitrogen) at its freezing point. The grid was transferred on a Gatan 626 cryoholder using a cryo-transfer device. After that it was transferred to a JEM-2010 TEM instrument. Direct imaging was carried out at a temperature of approximately −175 °C and with a 120 kV accelerating voltage, by use of the images acquired with a SC 1000 CCD camera (Gatan, Inc., Warrendale, PA).

AM1 calculations: AM1 calculations for **2a–d** and **3a** were carried out with the Gaussian 03 program[31] and either an HP Compaq dc5100 SFF computer or an HPC P4 Linux.

Acknowledgements

This work was supported by Grants-in-Aid for Young Scientists (B) (No. 17750137) and Scientific Research in a Priority Area "Super-Hier-

archical Structures" (Nos. 18039038, 19022036) from the Ministry of Education, Culture, Sports, Science and Technology (MEXT) and the "Academic Frontier" Project for Private Universities; namely the matching fund subsidy from the MEXT, 2003–2008, and the Ritsumeikan Global Innovation Research Organization (R-GIRO) project (2008–2013). The authors thank Prof. Tomohiro Miyatake, Ryukoku University, for FAB-MS measurements, Prof. Hiroshi Shinokubo, Nagoya University, and Prof. Atsuhiro Osuka, Kyoto University, for the ESI-TOF-MS measurements, and Dr. Ryugo Tero, Institute for Molecular Science (IMS), Prof. Munenori Numata, Kyoto Prefectural University, and Prof. Hitoshi Tamiaki, Ritsumeikan University, for helpful discussions. E.L. and M.L. thank the National Creative Research Initiative Program of the Korean Ministry of Science and Technology, and E.L. acknowledges a fellowship of the BK21 program from the Ministry of Education and Human Resources Development.

[1] D. Voet, J. G. Voet, *Biochemistry*, Wiley, New York, **2004**.

[2] a) J. N. Israelachvili, *Intermolecular and Surface Forces*, Academic Press, London, **1992**; b) I. W. Hamley, *Introduction of Soft Matter—Polymers, Colloids, Amphiphiles and Liquid Crystals*, Wiley, New York, **2000**.

[3] a) M. Lee, Y.-S. Jeong, B.-K. Cho, N.-K. Oh, W.-C. Zin, *Chem. Eur. J.* **2002**, *8*, 867–883; b) Y.-S. Yoo, J.-H. Choi, J.-H. Song, N.-K. Oh, W.-C. Zin, S. Park, T. Chang, M. Lee, *J. Am. Chem. Soc.* **2004**, *126*, 6294–6300; c) L.-Y. Jin, J.-H. Ahn, M. Lee, *J. Am. Chem. Soc.* **2004**, *126*, 12208–12209; d) D.-J. Hong, E. Lee, M. Lee, *Chem. Commun.* **2007**, 1801–1803; e) K.-S. Moon, H.-J. Kim, E. Lee, M. Lee, *Angew. Chem.* **2007**, *119*, 6931–6934; *Angew. Chem. Int. Ed.* **2007**, *46*, 6807–6810; f) E. Lee, Y.-H. Jeong, J.-K. Kim, M. Lee, *Macromolecules* **2007**, *40*, 8355–8360.

[4] a) J. P. Hill, W. Jin, A. Kosaka, T. Fukushima, H. Ichihara, T. Shimomura, K. Ito, T. Hashizume, N. Ishii, T. Aida, *Science* **2004**, *304*, 1481–1483; b) W. Jin, T. Fukushima, M. Niki, A. Kosaka, N. Ishii, T. Aida, *Proc. Natl. Acad. Sci. USA* **2005**, *102*, 10801–10806; c) W. Jin, T. Fukushima, A. Kosaka, M. Niki, N. Ishii, T. Aida, *J. Am. Chem. Soc.* **2005**, *127*, 8284–8285; d) J. Motoyanagi, T. Fukushima, N. Ishii, T. Aida, *J. Am. Chem. Soc.* **2006**, *128*, 4220–4221; e) Y. Yamamoto, T. Fukushima, Y. Suna, N. Ishii, A. Saeki, S. Seki, S. Tagawa, M. Taniguchi, T. Kawai, T. Aida, *Science* **2006**, *314*, 1761–1764; f) G. Zhang, W. Jin, T. Fukushima, A. Kosaka, N. Ishii, T. Aida, *J. Am. Chem. Soc.* **2007**, *129*, 719–722; g) J. L. Mynar, T. Yamamoto, T. A. Kosaka, T. Fukushima, N. Ishii, T. Aida, *J. Am. Chem. Soc.* **2008**, *130*, 1530–1531; h) T. Yamamoto, T. Fukushima, A. Kosaka, W. Jin, Y. Yamamoto, N. Ishii, T. Aida, *Angew. Chem.* **2008**, *120*, 1696–1699; *Angew. Chem. Int. Ed.* **2008**, *47*, 1672–1675.

[5] X. Zhang, Z. Chen, F. Würthner, *J. Am. Chem. Soc.* **2007**, *129*, 4886–4887.

[6] a) *Stimuli-Responsive Water Soluble and Amphiphilic Polymers* (Ed.: C. L. McCormick), ACS, Washington, **2001**; b) *Stimuli-Responsive Polymeric Films and Coating* (Ed.: M. W. Urban), ACS, Washington, **2005**; c) S. V. Aathimanikandan, E. N. Savariar, S. Thayumanavan, *J. Am. Chem. Soc.* **2005**, *127*, 14922–14929; d) S. Basu, D. R. Vutukuri, S. Thayumanavan, *J. Am. Chem. Soc.* **2005**, *127*, 16794–16795.

[7] a) H. Maeda, *Eur. J. Org. Chem.* **2007**, 5313–5325; b) H. Maeda, *Chem. Eur. J.* **2008**, *14*, 11274–11282; c) H. Maeda, *J. Incl. Phenom.* **2009**, unpublished results.

[8] a) H. Maeda, Y. Kusunose, *Chem. Eur. J.* **2005**, *11*, 5661–5666; b) C. Fujimoto, Y. Kusunose, H. Maeda, *J. Org. Chem.* **2006**, *71*, 2389–2394; c) H. Maeda, Y. Ito, *Inorg. Chem.* **2006**, *45*, 8205–8210; d) H. Maeda, Y. Ito, Y. Kusunose, *Chem. Commun.* **2007**, 1136–1138; e) H. Maeda, Y. Kusunose, Y. Mihashi, T. Mizoguchi, *J. Org. Chem.* **2007**, *72*, 2612–2616; f) H. Maeda, M. Terasaki, Y. Haketa, Y. Mihashi, Y. Kusunose, *Org. Biomol. Chem.* **2008**, *6*, 433–436; g) H. Maeda, Y. Fujii, Y. Mihashi, *Chem. Commun.* **2008**, 4285–4287; h) H. Maeda, Y. Haketa, Y. Bando, S. Sakamoto, *Synth. Met.* **2009**, *159*, in press.

[9] a) H. Maeda, Y. Haketa, T. Nakanishi, *J. Am. Chem. Soc.* **2007**, *129*, 13661–13674; b) H. Maeda, Y. Haketa, *Org. Biomol. Chem.* **2008**, *6*, 3091–3095; c) H. Maeda, Y. Mihashi, Y. Haketa, *Org. Lett.* **2008**, *10*, 3179–3182; d) H. Maeda, N. Eifuku, *Chem. Lett.* **2009**, *38*, in press.

[10] a) *Supramolecular Chemistry of Anions* (Eds.: A. Bianchi, K. Bowman-James, E. García-España), Wiley-VCH, Weinheim, **1997**; b) *Fundamentals and Applications of Anion Separations* (Eds.: R. P. Singh, B. A. Moyer), Kluwer Academic/Plenum Publishers, New York, **2004**; c) Anion Sensing (Ed.: I. Stibor), *Top. Curr. Chem.* **2005**, *Vol. 255*, edited by; d) J. L. Sessler, P. A. Gale, W.-S. Cho, *Anion Receptor Chemistry*, RSC, Cambridge, **2006**; e) Recognition of Anions (Ed.: R. Vilar): *Struct. Bonding* **2008**, *Vol. 129*.

[11] a) F. P. Schmidtchen, M. Berger, *Chem. Rev.* **1997**, *97*, 1609–1646; b) P. D. Beer, P. A. Gale, *Angew. Chem.* **2001**, *113*, 502–532; *Angew. Chem. Int. Ed.* **2001**, *40*, 486–516; c) R. Martínez-Mãnez, F. Sancenón, *Chem. Rev.* **2003**, *103*, 4419–4476; d) P. A. Gale, R. Quesada, *Coord. Chem. Rev.* **2006**, *250*, 3219–3244.

[12] a) C. B. Black, B. Andrioletti, A. C. Try, C. Ruiperez, J. L. Sessler, *J. Am. Chem. Soc.* **1999**, *121*, 10438–10439; b) P. Anzenbacher, Jr., A. C. Try, H. Miyaji, K. Jursikova, V. M. Lynch, M. Marquez, J. L. Sessler, *J. Am. Chem. Soc.* **2000**, *122*, 10268–10272; c) T. Mizuno, W.-H. Wei, L. R. Eller, J. L. Sessler, *J. Am. Chem. Soc.* **2002**, *124*, 1134–1135; d) J. L. Sessler, H. Maeda, T. Mizuno, V. M. Lynch, H. Furuta, *Chem. Commun.* **2002**, 862–863; e) J. L. Sessler, G. D. Pantos, E. Katayev, V. M. Lynch, *Org. Lett.* **2003**, *5*, 4141–4144; f) S. J. Coles, J. G. Frey, P. A. Gale, M. B. Hursthouse, M. E. Light, K. Navakhun, G. L. Thomas, *Chem. Commun.* **2003**, 568–569; g) I. El Drubi Vega, P. A. Gale, M. B. Hursthouse, M. E. Light, *Org. Biomol. Chem.* **2004**, *2*, 2935–2941; h) J. L. Sessler, G. D. Pantos, P. A. Gale, V. M. Lynch, *Org. Lett.* **2006**, *8*, 1593–1596; i) J. L. Sessler, D.-G. Cho, V. M. Lynch, *J. Am. Chem. Soc.* **2006**, *128*, 16518–16519.

[13] a) *Giant Vesicles* (Eds.: P. L. Luisi, P. Walde), Wiley-VCH, Weinheim, **2000**; b) A. Shioi, T. A. Hatton, *Langmuir* **2002**, *18*, 7341–7348; c) Z. Li, M. A. Hillmyer, T. P. Lodge, *Nano Lett.* **2006**, *6*, 1245–1249.

[14] N. C. Johnson, G. Stemp, N. Anand, C. S. Stephen, T. Gallagher, *Synlett* **1998**, 1025–1027.

[15] a) B. Oddo, C. Dainotti, *Gazz. Chim. Ital.* **1912**, *42*, 716–726; b) W. M. Stark, M. G. Baker, F. J. Leeper, P. R. Raithby, A. R. Battersby, *J. Chem. Soc. Perkin Trans. 1* **1988**, 1187–1201.

[16] For example: a) Y. Zheng, Y.-Y. Won, F. S. Bates, H. T. Davis, L. E. Scriven, Y. Talmon, *J. Phys. Chem. B* **1999**, *103*, 10331–10334; b) E. E. Dormidontova, *Macromolecules* **2002**, *35*, 987–1001; c) Z. Li, E. Kesselman, Y. Talmon, M. A. Hillmyer, T. P. Lodge, *Nature* **2004**, *427*, 98–101.

[17] In the case of the tetra-TEG-substituted **2b**, smaller emissions in the red-shift region (λ_{em} = 722 and 808 nm) are also observed by excitation at 460 nm in an aqueous solution. The excitation spectra for these emission maxima exhibit the λ_{max} values of 475 and 479 nm, respectively, with the shoulder around 500 nm. Such blue-shifted excitation spectra, which differ from those for the emission of monomers at 546 nm, appear to be derived from the H-aggregates themselves (in the Supporting Information Figure S14).

[18] The DLS data have been corrected by using the parameters of viscosity and reflectivity of the solvent. The averaged values of five measurements for each molecule at 70 °C are shown in the manuscript. The awkward behaviors of the amphiphiles at 20 °C in aqueous solutions are possibly due to the geometries of the organized structures that are far from the spheres in some cases. As of this moment, by using DLS measurements, we can suggest the formation of the nanometer-scale assemblies from the amphiphilic anion receptors.

[19] As the example of freeze-drying to be used in order to sustain the structures in aqueous solutions: S. R. Bull, L. C. Palmer, N. J. Fry, M. A. Greenfield, B. W. Messmore, T. J. Meade, S. I. Stupp, *J. Am. Chem. Soc.* **2008**, *130*, 2742–2743.

[20] Cryo-TEM measurement of **3b** also suggests the formation of cylindrical aggregates (in the Supporting Information Figure S18).

Table 1. Binding constants (K_a, M^{-1}) of the PEG-substituted receptors **2a–d**, **3a**, and **3b**, and reference **1a** with various anions as TBA salts in CH_2Cl_2[a].

	Cl^-	Br^-	$CH_3CO_2^-$	$H_2PO_4^-$	HSO_4^-
2a	20000 (0.67)	2000 (0.71)	290000 (1.4)	6200 (0.09)	210 (0.39)
2b	29000 (0.97)	2500 (0.89)	210000 (1.0)	200000 (2.8)	1200 (2.2)
2c	47000 (1.6)	3300 (1.2)	200000 (0.95)	360000 (5.0)	1900 (3.5)
2d	14000 (0.47)	1200 (0.43)	190000 (0.90)	360000 (5.0)	440 (0.81)
3a	37000 (1.2)	3800 (1.4)	780000 (3.7)	190000 (2.6)	710 (1.3)
3b	26000 (0.87)	2600 (0.93)	350000 (1.7)	300000 (4.2)	380 (0.70)
1a[b]	30000	2800	210000	72000	540

[a] The values in the parentheses are the ratios to K_a of **1a**. [b] Ref. [9a].

[21] Solvent-aided control of functional nanostructures have been reported: a) J.-K. Kim, E. Lee, M. Lee, *Angew. Chem.* **2006**, *118*, 7353–7356; *Angew. Chem. Int. Ed.* **2006**, *45*, 7195–7198; b) S. Yagai, M. Ishii, T. Karatsu, A. Kitamura, *Angew. Chem.* **2007**, *119*, 8151–8155; *Angew. Chem. Int. Ed.* **2007**, *46*, 8005–8009.

[22] For selected recent examples of temperature-dependent stacking assemblies: a) P. Jonkheijm, P. van der Schoot, A. P. H. J. Schenning, E. W. Meijer, *Science* **2006**, *313*, 80–84; b) X.-Q. Li, V. Stepanenko, Z. Chen, P. Prins, L. D. A. Siebbeles, F. Würthner, *Chem. Commun.* **2006**, 3871–3873; c) F. J. M. Hoeben, M. Wolffs, J. Zhang, S. De Feyter, P. Leclère, A. P. H. J. Schenning, E. W. Meijer, *J. Am. Chem. Soc.* **2007**, *129*, 9819–9828; d) K. P. van den Hout, R. Martín-Rapún, J. A. J. M. Vekemans, E. W. Meijer, *Chem. Eur. J.* **2007**, *13*, 8113–8123; e) Z. Tomović, J. van Dongen, S. J. George, H. Xu, W. Pisula, P. Leclère, M. M. J. Smulders, S. De Feyter, E. W. Meijer, A. P. H. J. Schenning, *J. Am. Chem. Soc.* **2007**, *129*, 16190–16196; f) Z. Chen, V. Stepanenko, V. Dehn, P. Prins, L. D. A. Siebbeles, J. Seibt, P. Marquetand, V. Engel, F. Würthner, *Chem. Eur. J.* **2007**, *13*, 436–449; g) V. Dehm, Z. Chen, U. Baumeister, P. Prins, L. D. A. Siebbeles, F. Würthner, *Org. Lett.* **2007**, *9*, 1085–1088; h) M. M. J. Smulders, A. P. H. J. Schenning, E. W. Meijer, *J. Am. Chem. Soc.* **2008**, *130*, 606–611; i) H. Wang, T. E. Kaiser, S. Uemura, F. Würthner, *Chem. Commun.* **2008**, 1181–1183.

[23] Recently, a temperature-dependent transformation between J- and H-aggregates from perylene bisimide dyes has been reported: S. Yagai, T. Seki, T. Karatsu, A. Kitamura, F. Würthner, *Angew. Chem.* **2008**, *120*, 3415–3419; *Angew. Chem. Int. Ed.* **2008**, *47*, 3367–3371.

[24] a) Association constants (K_a) of **2a–d**, **3a**, and **3b** for anions in the *organic solvent* (CH_2Cl_2) estimated by UV/Vis absorption spectral changes upon the addition of anions as tetrabutylammonium (TBA) salts are summarized in Table 1. The absorption maxima λ_{max} are hardly shifted (less than 6 nm) by the binding anions, and the intensity is moderately decreased. Further, the K_a values of **2a–d**, **3a**, and **3b** for Cl^- and Br^- are comparable to those of α-phenyl-substituted **1a**. In contrast to the fairly suppressed K_a of **2a** for $H_2PO_4^-$, those of **2b–d**, **3a**, and **3b** are significantly enhanced as compared to those of **2a** as well as **1a**, possibly due to the stabilization of the polarized acidic moieties of the oxoanions by hydrogen-bonding-accepting TEG substituents. Other oxoanions, $CH_3CO_2^-$ and HSO_4^-, have the comparable or augmented K_a values depending on the receptors (in the Supporting Information Figure S2–10); b) K_a values for **3c** and **d** have not been determined because they cannot form the assemblies in aqueous solutions because of their insolubility.

[25] Similar to the stable assemblies in aqueous solutions, J-type (**3a** and **3b**) and H-type assemblies (**3c**,**d**) in hexane (1×10^{-5} M) appear to be sustainable to anions (e.g. Cl^- as a TBA salt), as examined by the UV/Vis absorption spectral changes between 60 and −60 °C.

[26] The DLS measurements exhibit the average sizes of ca. 170 (**2c**) and 180 (**3a**) nm at 20 °C, which may not be exact values due to the "mixture" solvent, CH_2Cl_2-saturated aqueous solutions but suggest the formation of fairly discrete assemblies.

[27] To an aqueous solution of the amphiphiles (e.g. **3a**), the addition of hexane and extraction afford the emulsion state, including the amphiphiles, between the organic (hexane) and aqueous phases, both of which are colorless and completely exclude the receptor **3a**. The UV/Vis absorption spectrum of the emulsion appears like that in hexane solution. The molecular-level "structures" in emulsion are also fascinating and are under investigation.

[28] G. C. Dol, P. C. J. Kamer, P. W. N. M. van Leeuwen, W. Qiu, *Eur. J. Org. Chem.* **1998**, 359–364.

[29] H. Lee, D. Kim, H.-K. Lee, W. Qiu, N.-K. Oh, W.-C. Zin, K. Kim, *Tetrahedron Lett.* **2004**, *45*, 1019–1022.

[30] C. N. Johnson, G. Stemp, N. Anand, S. C. Stephen, T. Gallagher, *Synlett* **1998**, 1025–1027.

[31] Gaussian 03, Revision C.01 and D.02, M. J. Frisch, G. W. Trucks, H. B. Schlegel, G. E. Scuseria, M. A. Robb, J. R. Cheeseman, J. A. Montgomery, Jr., T. Vreven, K. N. Kudin, J. C. Burant, J. M. Millam, S. S. Iyengar, J. Tomasi, V. Barone, B. Mennucci, M. Cossi, G. Scalmani, N. Rega, G. A. Petersson, H. Nakatsuji, M. Hada, M. Ehara, K. Toyota, R. Fukuda, J. Hasegawa, M. Ishida, T. Nakajima, Y. Honda, O. Kitao, H. Nakai, M. Klene, X. Li, J. E. Knox, H. P. Hratchian, J. B. Cross, C. Adamo, J. Jaramillo, R. Gomperts, R. E. Stratmann, O. Yazyev, A. J. Austin, R. Cammi, C. Pomelli, J. W. Ochterski, P. Y. Ayala, K. Morokuma, G. A. Voth, P. Salvador, J. J. Dannenberg, V. G. Zakrzewski, S. Dapprich, A. D. Daniels, M. C. Strain, O. Farkas, D. K. Malick, A. D. Rabuck, K. Raghavachari, J. B. Foresman, J. V. Ortiz, Q. Cui, A. G. Baboul, S. Clifford, J. Cioslowski, B. B. Stefanov, G. Liu, A. Liashenko, P. Piskorz, I. Komaromi, R. L. Martin, D. J. Fox, T. Keith, M. A. Al-Laham, C. Y. Peng, A. Nanayakkara, M. Challacombe, P. M. W. Gill, B. Johnson, W. Chen, M. W. Wong, C. Gonzalez, J. A. Pople, Gaussian, Inc., Wallingford CT, **2004**.

Received: October 17, 2008
Published online: February 16, 2009

